Geology and setting of the Red Mountain gold-silver deposits, northwestern British Columbia

D.A. RHYS, M. SIEB, S.R. FROSTAD, C.L. SWANSON and M.A. PREFONTAINE
Lac Minerals Ltd., Red Mountain Project, Stewart, British Columbia

J.K. MORTENSEN
Department of Geological Sciences, The University of British Columbia, Vancouver, British Columbia

H.Q. SMIT
Lac Minerals Ltd., Red Mountain Project, Stewart, British Columbia

ABSTRACT

Gold-silver mineralization at Red Mountain (1992 resource of 2.5 million tonnes grading 12.8 g/t Au and 38.1 g/t Ag) occurs within several discrete zones within a folded sequence of Middle to Late Triassic Triassic sedimentary rocks, Early Jurassic volcaniclastic and pyroclastic rocks, and Early Jurassic intrusions. Three phases of Early Jurassic sills and stocks collectively comprise the Goldslide intrusions: (1) irregular bodies of medium-grained hornblende monzodiorite (Hillside porphyry); (2) hornblende-biotite + quartz porphyritic monzodiorite to quartz monzodiorite (Goldslide porphyry; U-Pb zircon ages of 197.1 + 1.9 Ma); and (3) biotite porphyritic hornblende monzodiorite sills (Biotite porphyry). Contact breccias and igneous breccia dikes are common features of the Goldslide intrusions. Chemical similarities and equivalent ages of volcanic rocks and intrusions, and the presence of intrusive clasts in volcanic rocks suggest that the intrusions are feeders to overlying volcanic units.

Hydrothermal alteration affects all pre-Tertiary rocks on Red Mountain, including all phases of the Goldslide intrusions. Several shallow-dipping alteration zones are developed sequentially above a propylitic quartz stockwork/molybdenum zone. These include: (1) sericite-quartz-pyrite alteration (pyrite-dominant alteration); (2) chlorite-K-feldspar-sericite-titanite alteration with disseminated and vein pyrrhotite (pyrrhotite-dominant alteration); and (3) brown to black tourmaline veins and K-feldspar-pyrite-titanite-actinolite alteration. Anomalous gold (>0.3 g/t) mineralization is developed at the transition from the pyrite to the pyrrhotite dominant alteration over a >1 km² area. Within this anomalous zone, high-grade (3 g/t to 20 g/t Au) gold-silver mineralization occurs in 5 m to 29 m thick, semi-tabular pyrite + pyrrhotite stockworks with intense sericitic alteration and surrounding disseminated sphalerite + pyrrhotite.

Stratigraphic, spatial and geochronologic relations and alteration zoning indicate that mineralization formed in a subvolcanic environment at the top of the Goldslide intrusions and at the base of the Early Jurassic volcanic pile. The Goldslide porphyry is interpreted to be the mineralizing intrusion. The alteration zoning, molybdenum-copper mineralized quartz stockworks, extensive K-silicate and tourmaline alteration, and the relationship with a hypabyssal porphyritic intrusion show similarities to many porphyry systems.

Introduction

Gold-silver mineralization is spatially associated with a suite of Early Jurassic intrusive rocks on Red Mountain, near Stewart, British Columbia. The mineralized zones occur within a broad area of zoned alteration. This paper describes the geology, mineralization and alteration at Red Mountain and is based on work by the authors and others during exploration of the property mainly during 1993 and 1994. The only previously published work on Red Mountain is a preliminary summary of the geology and a report of several ^{40}Ar-^{39}Ar dates for the Goldslide and other intrusions in Schroeter et al. (1992). Brief descriptions of the host strata and intrusions and observations bearing on the timing of mineralization are given in a regional geologic context by Greig et al. (1994a, 1994b), and a U-Pb age for a sill of the Goldslide intrusions is given by Greig et al. (1995).

Red Mountain is situated at the southeastern end of the Bitter Creek valley, 15 km east of Stewart, British Columbia (Fig. 1). It is bounded on the east by the Cambria Icefield and on the south and west by the Bromley Glacier and its tributaries (Fig. 2). The area is characterized by steep terrain and local elevations range from 550 m at the toe of the Bromley Glacier to 2129 m at the peak of Red Mountain. Access is currently by helicopter from Stewart. An access road was constructed to within 4 km of the mountain in 1994. A proposal to continue the road to a location just north of the toe of Bromley Glacier and install a tram to provide access to higher elevations where ore zones are located is currently on hold.

History

A few small adits in the upper part of the Bitter Creek valley, such as on Hartley Gulch and the east side of Mt. Dickie, attest to the work of prospectors in the first half of this century. At that time, snowfields probably covered much of Red Mountain, and the Bromley Glacier extended over 3 km further down the valley.

The large gossan covering Red Mountain attracted exploration for porphyry-molybdenum deposits during the late 1960s. Prospecting and drilling (700 m) tested porphyry-style molybdenum mineralization in the Red Mountain cirque near the present exploration camp and on the southwest side of the mountain at McAdam Point (Reeve, 1967; Grove, 1968). Reconnaissance programs run by Zenore Resources and by Falconbridge Nickel Mines Ltd. further evaluated the molybdenum potential of the area in the late 1970s (Downing and Leitch, 1980).

In 1988 and 1989, Wotan Resources staked claims over Red Mountain, and in 1989, Bond Gold Canada Inc. optioned the property to evaluate its gold potential. During the early part of the 1989 program, Marc Gauthier, a draftsman for Bond Gold, collected the first high-grade gold samples from what was to become the Marc zone, in an area that was probably covered by snow a decade earlier. On the basis of the Marc zone discovery, and several other gold-silver showings found on the mountain, Bond Gold initiated a major exploration program in 1989. During the period from 1989 to 1991, a total of 19 783 m was drilled in 89 diamond

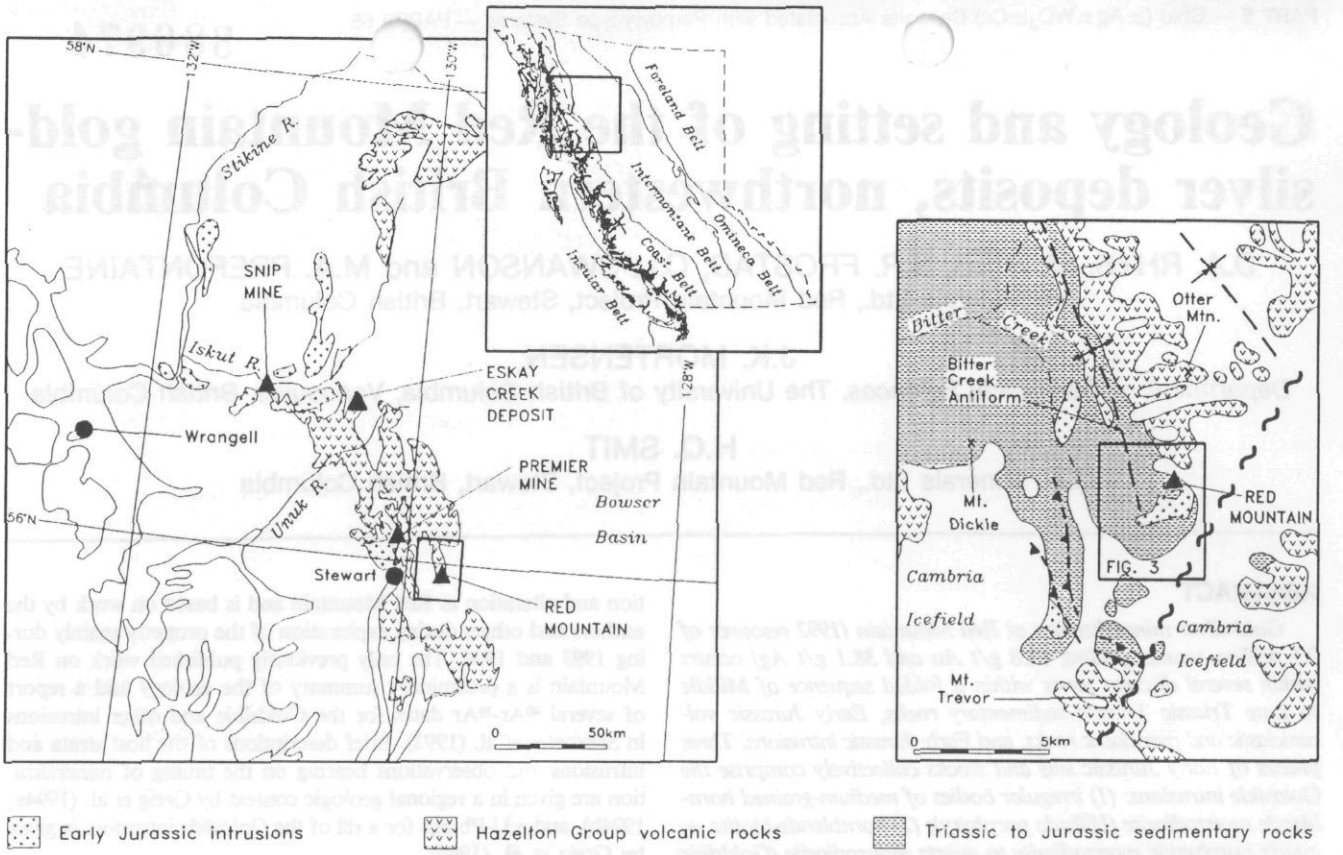

FIGURE 1. Location of Red Mountain in northwestern British Columbia. Other significant gold deposits in the area (left), the regional distribution of Early Jurassic intrusions and Hazelton Group rocks, and the location of Figure 3 (right) are shown. The diagram at the right is after Greig et al. (1994a, 1994b).

drill holes, most of which were to define the Marc zone. Geological mapping, sampling, and airborne, surface and downhole geophysical surveys were also undertaken at this time. Bond Gold was purchased by Lac Minerals Ltd. in early 1991.

By the end of 1991, discontinuous north-south trending mineralization comprising two main lenses was postulated for the Marc zone. A reinterpretation by John Watkins in early 1992 suggested that mineralization followed a northwest-southeast trend and that there were two continuous zones, the Marc and the AV, with the more northerly AV zone remaining open. A 4000 m, 13-hole drilling program in 1992 confirmed this interpretation, and at the end of 1992 a resource of 2.5 million tonnes grading 12.8 g/t Au and 38.1 g/t Ag was estimated for the property (Lac Minerals Ltd., May 1993 Red Mountain Project Prospectus). The potential for a major deposit was apparent, and Lac Minerals Ltd. initiated an extensive exploration program in 1993 under the direction of Garfield MacVeigh to bring this resource into reserve categories and to explore for additional mineralization. As well, a prospectus was submitted to the British Columbia government and technical and environmental studies required to acquire a mine development certificate were accelerated.

In 1993 and 1994, 1315 m of underground development were completed in the Marc and AV zone area. This included a decline in the Marc footwall and AV hangingwall, 21 drill stations, and three cross-cuts through the Marc zone. A total of 76 503 m was drilled in 304 diamond drill holes from surface and underground. Definition drilling was undertaken on the Marc and AV zones. Drilling also discovered and evaluated the 141 and JW zones and explored other geophysical and geological targets on the property. Underground bulk sampling, geological mapping, geophysics and geochemical studies were also undertaken. The property is currently owned by Barrick Gold Corp. as a result of its September 1994 takeover of Lac Minerals Ltd.

Exploration Techniques

The Marc zone was discovered by sampling below a small rusty, highly-altered cliff. Since then, a wide variety of exploration techniques have been used on the mountain, including: (1) prospecting; (2) geological mapping; (3) airborne, surface and down-hole geophysics; (4) rock, talus and soil geochemistry; (5) diamond drilling; (6) underground development and sampling; and (6) bulk sampling. The AV and JW zones were found by drilling the strike projection of the Marc zone. The 141 zone was discovered by a drill hole targeted deep on the AV zone.

Geophysical responses include areas of strong chargeability, low resistivity in areas of widespread pyrrhotite mineralization, differences in magnetic susceptibility over different rock types, a broad UTEM response over a sphalerite- and pyrrhotite-rich halo to the Marc zone and discrete I.P. responses from areas containing pyrrhotite. Some of these areas have significant gold values, but no large mineralized zones have been found to date using geophysics. In general, geophysical responses from the widespread sulphide mineralization and alteration zones do not allow discrimination of relatively smaller high-grade sulphide zones.

Rock, talus, soil and drill core samples have been analyzed by assay, ICP and whole rock methods. As with geophysics, geochemistry is an important tool for delineating alteration zones and outlining broad areas which are favourable for gold mineralization. However, detailed geology and drilling within these areas is required to find potential ore zones. Due to variability of gold grades and a lack of distinctive structural or lithologic hosts, relatively close-spaced drilling and underground development is required to upgrade zones from a resource into mineral inventories. Additional exploration targets on Red Mountain will likely result from a careful analysis of geology and geochemistry to outline areas which are favourable for high grade mineralization.

Regional Geologic Setting

Red Mountain is located near the western margin of the Stikine terrane in the Intermontane Belt (Fig. 1). Three principal stratigraphic elements are recognized in Stikinia and are present in the Stewart area: (1) Middle and Upper Triassic clastic rocks and chert of the Stuhini Group; (2) Lower and Middle Jurassic volcanic and clastic rocks of the Hazelton Group; and (3) Upper Jurassic mudstone, siltstone and sandstone of the Bowser Lake Group (Anderson, 1993; Greig et al., 1994a; Fig. 1). Rocks of the former two packages, together with Early Jurassic intrusive rocks that are common to this part of Stikinia, host the Red Mountain deposit (Figs. 1, 3; Greig et al., 1994a, 1994b). Preservation of primary volcanic textures and sedimentary structures, together with metamorphic mineral assemblages consisting of common chlorite, $CaCO_3$, epidote and rare fine-grained actinolitic amphibole suggest that regional metamorphic grade is probably sub-greenschist to lowermost greenschist facies (C. Greig, pers. comm., 1995).

Intrusive rocks in the region have been subdivided into several plutonic suites that range in age from Late Triassic to Eocene (Anderson, 1993; Greig et al., 1994a). The Stikine plutonic suite comprises Late Triassic calc-alkaline intrusions which are coeval with Stuhini Group volcanic rocks. Early to Middle Jurassic plutons are variable in composition, are roughly coeval and cospatial with Hazelton Group volcanic rocks, and are metallogenically important. Intrusions of Eocene age occur in the Coast Belt to the west and south of Red Mountain (Carter, 1981; Greig et al., 1994b, 1995).

Red Mountain occurs within the disrupted core of the northwest-trending Bitter Creek antiform (Fig. 1; Greig et al., 1994a, 1994b), a complex structure traceable for at least 20 km along the eastern side of the Bitter Creek valley. On its eastern limb is a thick sequence of broadly folded, generally east-dipping and east-facing, predominantly volcanic rocks of the Early Jurassic Hazelton Group, and on its western limb are tightly folded, predominantly west-dipping and west-facing, Middle Triassic to Lower Jurassic sedimentary strata. The voluminous rocks of the eastern limb of the Bitter Creek antiform are not observed on its western limb; this suggests disruption by faulting and/or localization along an Early Jurassic facies boundary.

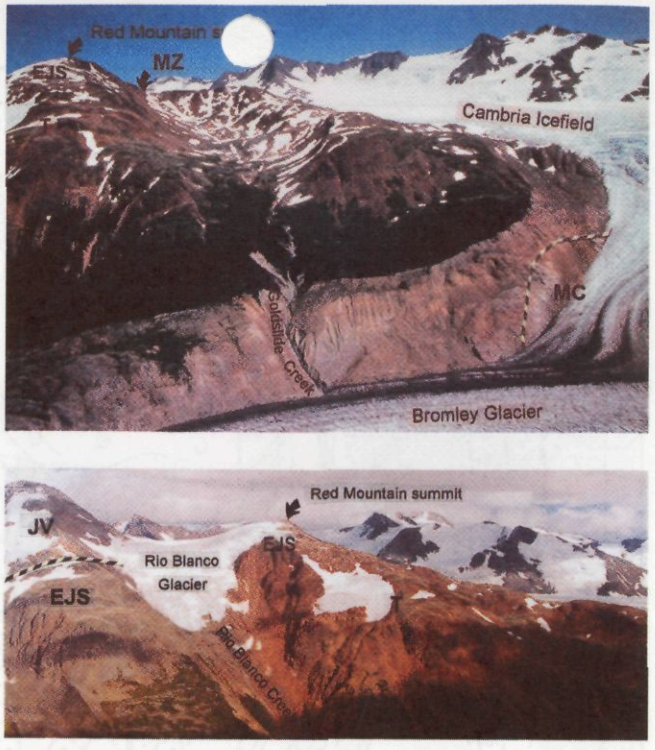

FIGURE 2. Aerial views of Red Mountain, looking east from approximately 3 km west of the mountain.
Top: View into the Red Mountain cirque showing the summit, location of the Marc zone surface showing (MZ), Bromley glacier and Goldslide Creek (center). The McAdam Point stock (MC), Triassic cherty sedimentary rocks (T) and Early Jurassic sedimentary rocks (EJS), including clastic and and volcaniclastic lithologies, are marked.
Bottom: A view taken approximately 2 km north of the previous photograph, looking up Rio Blanco Creek. Red Mountain summit is in the centre and the cirque is at the right. Triassic cherty sedimentary rocks (T) and Early Jurassic clastic and subordinate volcaniclastic strata (EJS) are marked. These are overlain by easterly-dipping Early Jurassic green and maroon volcanic and volcaniclastic rocks (JV) in the top left corner of the photograph. Sills of Biotite porphyry intrude most of the visible Triassic and basal Jurassic strata. Note the abrupt termination of the gossan at Rio Blanco Creek.

Geology of Red Mountain

Red Mountain is underlain by folded Middle to Upper Triassic and Early Jurassic sedimentary and minor volcanic strata that are intruded by Early Jurassic plutons, sills and dikes known as the Goldslide intrusions, and by Tertiary intrusions (Fig. 3).

Stratified rocks comprise a sequence of Triassic chert and fine-grained siliciclastic rocks, which underlie much of the mountain that are gradationally overlain by Early Jurassic clastic and volcaniclastic rocks. The Triassic sequence consists of massive to thinly bedded, grey, white and pale green cherty siltstone, mudstone and chert. These rocks occur on the west side of Red Mountain north of Goldslide Creek, throughout the south ridge, and as screens in the Goldslide intrusions within the Red Mountain cirque (Fig. 3). Bedding is defined by colour banding or laminae of chert and grey to green mudstone. Thin (generally <50 cm), lenses of recrystallized grey limestone occur locally. Dark grey to black, commonly carbonaceous and/or calcareous mudstone, siltstone and chert predominate on the far western and southern sides of Red Mountain (Fig. 3) and overlie the grey cherty rocks. These strata are locally interbedded and interfinger with the grey cherty lithologies. Interbeds of dark grey cherty siltstone in grey chert collected from several localities approximately 500 m north of the exploration camp (Fig. 3) yielded radiolaria whose ages range from Ladinian to Norian, thus establishing a Middle to Late Triassic age for the lower sequence (Cordey and Greig, 1995).

A massive green to grey, tuffaceous fine- to medium-grained rock of uncertain lithologic type underlies a large portion of the south ridge (Fig. 3). The unit comprises 20% to 35% medium-grained plagioclase and 1% to 5% mafic minerals, generally biotite and hornblende, in a poorly sorted matrix. Grains are commonly ragged and broken, but are locally subhedral. The unit commonly contains angular fragments of cherty siltstone, and at its northeast end grades into a mud-chip breccia with 5% to 25% fragments of grey cherty mudstone (Fig. 3). The breccia is locally well-bedded, and has graded bedding, suggesting that it is a tuff or a sedimentary rock. However, discordant contacts of the massive tuffaceous unit with bedded sedimentary rocks elsewhere on the south ridge may suggest an intrusive origin.

The Triassic chert and fine-grained siliciclastic strata are overlain by Lower Jurassic clastic, volcaniclastic and volcanic rocks. These strata occur on the north and northeastern side of Red Mountain (Figs. 2 and 3). Although stratigraphic relationships with the underlying Triassic cherty rocks are complicated due to faulting, folding, alteration and the presence of numerous intrusions, the Early Jurassic strata appear to grade downward into the Triassic rocks. Green to grey laminated siltstone, mudstone, fine-grained greywacke and, locally, conglomerate and agglomerate, occur at the Red Mountain summit and north of Rio Blanco and comprise the base of the upper sequence (Figs. 2 and 3). The clastic rocks at the Red Mountain summit locally contain bivalves which are of probable Early Jurassic age (J. Palfy, pers. comm., 1994). Cross-bedding, load structures and graded bedding in the siltstones and sandstones indicate an overall east to northeast-facing direction to the Early Jurassic package. Conglomerates contain rounded to

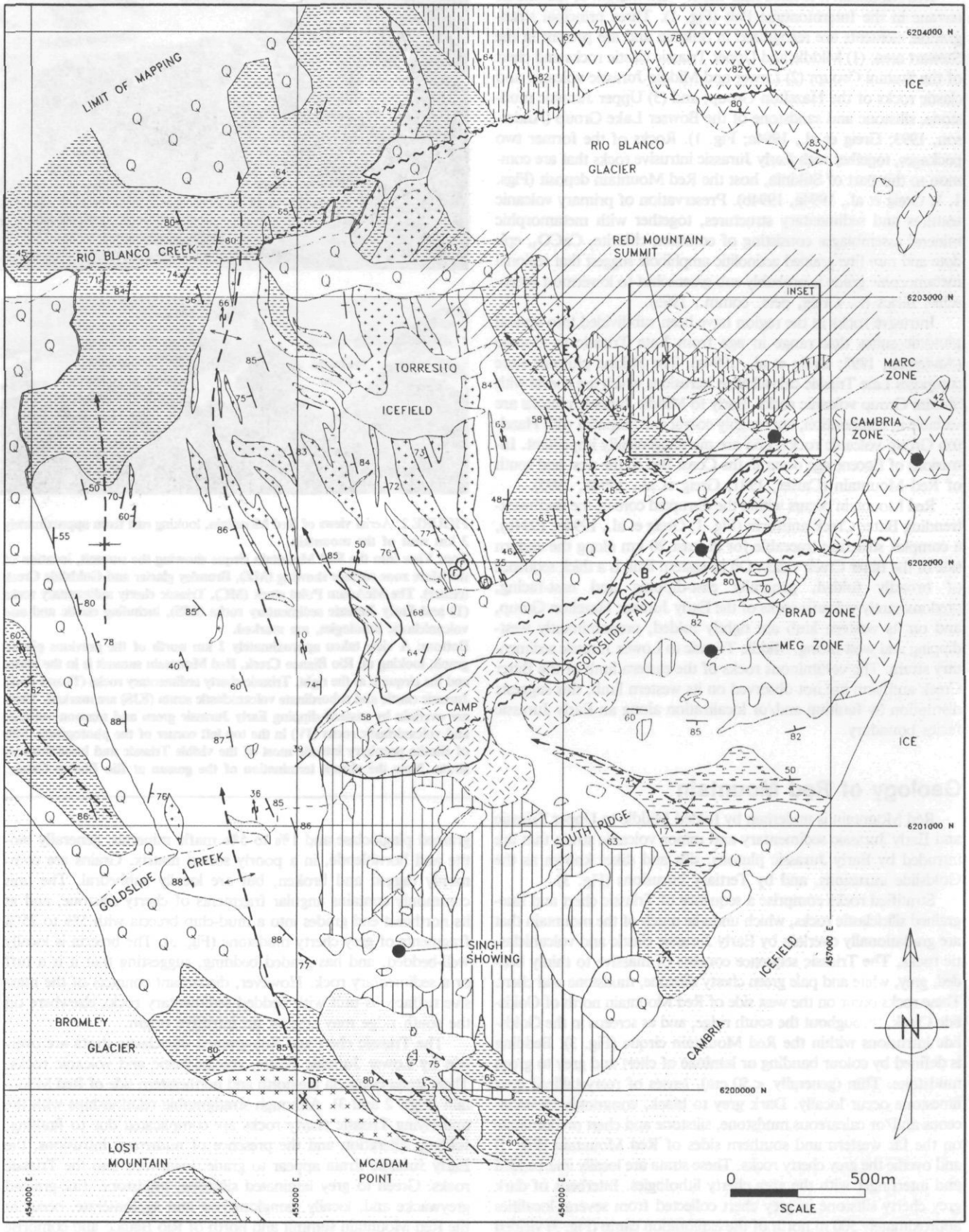

FIGURE 3a. Geology of the Red Mountain area, northwestern British Columbia. Map location is shown on Figure 1. Note that the locations of radiolarian fossil localities (Cordey and Greig, 1995) and age date samples (A, C and D from Schroeter et al., 1992; E from Greig et al., 1995) are shown.

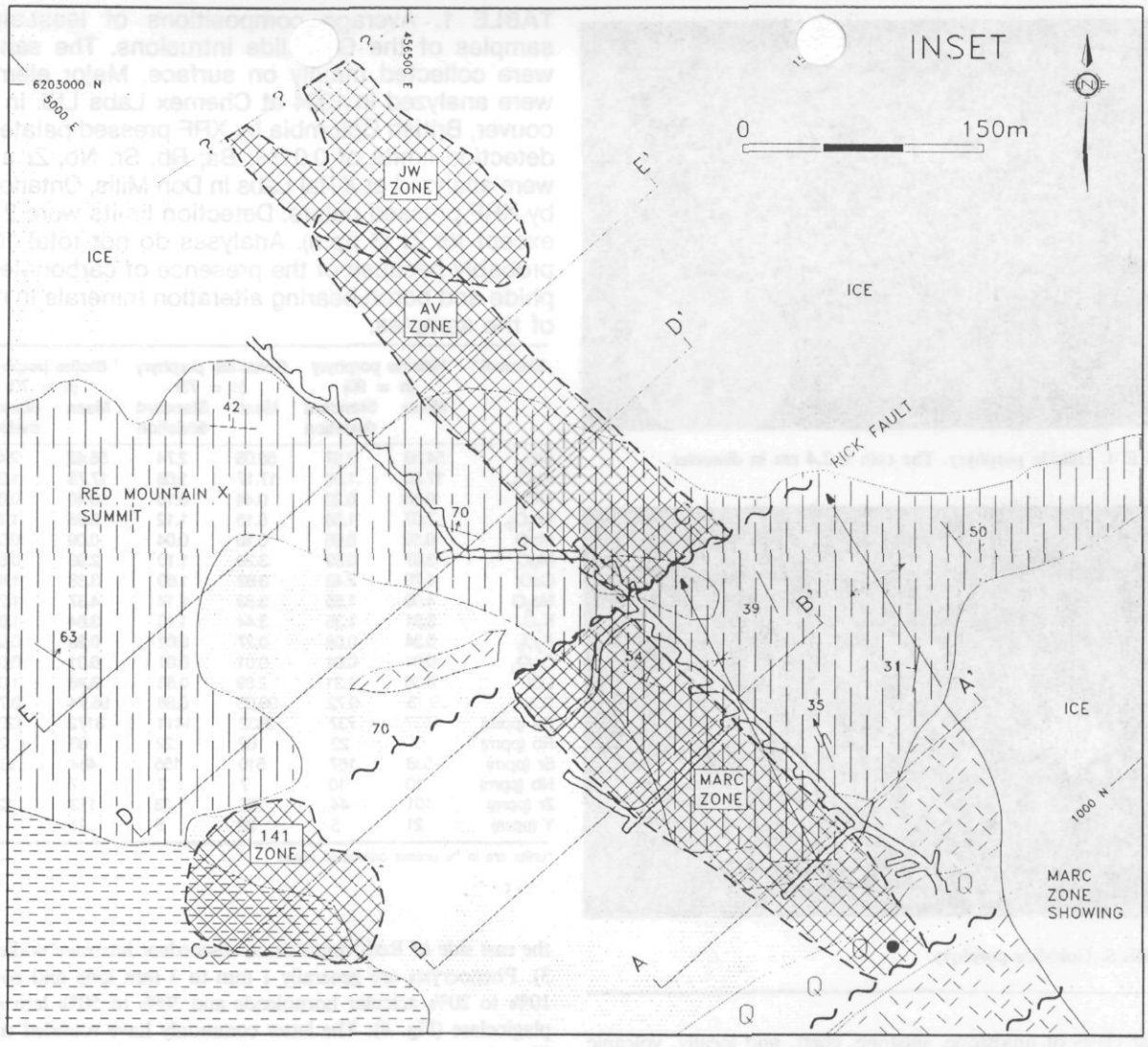

LEGEND

Q Talus and moraine

SEDIMENTARY AND VOLCANIC ROCKS

Early Jurassic

- Maroon tuff and volcanic conglomerate.
- Green conglomerate, tuff and siltstone.
- Green to grey siltstone, greywacke and conglomerate.

Middle to upper Triassic

- Dark grey to black locally graphitic mudstone, siltstone and chert.
- Bedded grey cherty siltstone, mudstone and chert.
- Bedded to massive grey chert breccia.

INTRUSIVE ROCKS

Tertiary: McAdam Point stock

- Biotite quartz monzonite, k-feldspar megacrystic.

Early Jurassic: Goldslide intrusions

- Hillside porphyry: fine to medium-grained hornblende monzodiorite.
- Goldslide porphyry: hornblende + biotite ± quartz porphyritic monzodiorite.
- Biotite porphyry: biotite prophyritic hornblende monzodiorite.

Uncertain affinity

- Massive green to grey tuffaceous rock

- Geologic contact
- Fault
- Bedding: tops unknown, tops known, overturned
- Anticline, syncline
- Minor fold, showing asymmetry
- Slaty to phyllitic foliation
- Area of quartz stockwork
- Area of most intense alteration and ·0.3 g/t anomalous gold
- Underground workings, inset only
- A A' Locations of cross-sections, inset only
- A Ar-Ar, 160 ± 5 Ma
- B U-Pb zircon sample #94-DR-421, 197.1 ± 1.9 Ma
- C Ar-Ar, 200 Ma
- D Ar-Ar, 45 ± 2 Ma
- E U-Pb zircon, 201.8 ± 0.5 Ma
- Ⓕ Radiolarian fossil localities

FIGURE 3b. The inset shows the surface projection of the ore zones and underground workings, surface geology, mine grid and location of cross sections in Figure 10. The contact between Triassic and Jurassic strata is approximate and gradational.

FIGURE 4. Hillside porphyry. The coin is 2.4 cm in diameter.

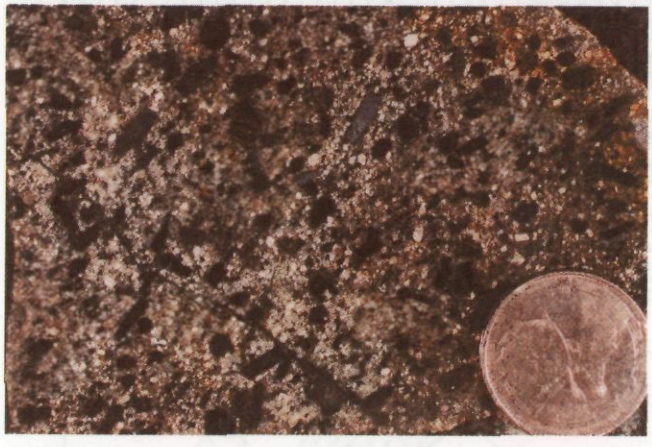

FIGURE 5. Goldslide porphyry.

TABLE 1. Average compositions of least-altered samples of the Goldslide intrusions. The samples were collected mainly on surface. Major elements were analyzed in 1994 at Chemex Labs Ltd. in Vancouver, British Columbia by XRF pressed palate with detection limits of 0.01%. Ba, Rb, Sr, Nb, Zr and Y were analyzed at X-Ral Labs in Don Mills, Ontario also by XRF pressed palate. Detection limits were 2 ppm except for Zr (3 ppm). Analyses do not total 100%, probably because of the presence of carbonate, sulphide and boron-bearing alteration minerals in many of the samples.

Element*	Hillside porphyry (n = 90)		Goldslide porphyry (n = 73)		Biotite porphyry (n = 70)	
	Mean	Standard deviation	Mean	Standard deviation	Mean	Standard deviation
SiO_2	54.89	3.97	58.06	2.74	56.42	2.44
Al_2O_3	17.20	1.36	17.17	1.06	17.73	1.21
TiO_2	0.58	0.20	0.44	0.10	0.40	0.08
Fe_2O_3	7.07	1.56	6.15	1.12	5.98	1.19
MnO	0.10	0.05	0.10	0.04	0.09	0.05
MgO	3.57	0.80	3.20	1.10	2.98	0.53
CaO	4.70	2.43	3.62	1.60	3.38	1.48
Na_2O	4.06	1.55	3.83	1.14	4.37	1.25
K_2O	3.31	1.35	3.44	1.10	3.64	1.02
P_2O_5	0.34	0.08	0.27	0.02	0.28	0.03
Cr_2O_3	0.01	0.01	0.01	0.01	0.01	0.01
LOI	3.30	1.31	2.89	0.86	3.46	1.05
Total	99.13	0.72	99.05	0.86	98.74	0.77
Ba (ppm)	1637	737	2632	1411	3172	1201
Rb (ppm)	64	22	62	22	66	22
Sr (ppm)	538	167	510	155	464	132
Nb (ppm)	10	10	7	2	7	1
Zr (ppm)	101	44	102	33	113	127
Y (ppm)	21	5	20	5	21	4

*units are in % unless otherwise noted

angular clasts of mudstone, siltstone, chert, and locally, volcanic rocks, in a poorly sorted coarse greywacke matrix. Rounded to subangular clasts of hornblende and biotite porphyritic monzodiorite that are texturally, mineralogically and chemically similar to phases of the Goldslide intrusions (see below) are abundant in some conglomerate and agglomerate beds on the north side of Rio Blanco, near Red Mountain summit and in extensive debris flow conglomerates that occur in the Cambria zone (Fig. 3). Agglomerate beds with pyroxene porphyritic volcanic clasts occur locally west of Red Mountain summit. These clastic and volcaniclastic lithologies are conformably overlain by interbedded green and maroon andesite to trachyandesite tuff, tuff breccia, volcanic conglomerate and subordinate siltstone, greywacke and possible andesitic flows that occur north of Red Mountain across Rio Blanco glacier (Fig. 3). Locally developed accretionary lapilli in maroon tuffs suggest that some of the volcanic rocks are subaerial ashfall tuffs.

Early Jurassic Intrusive Rocks on Red Mountain: The Goldslide Intrusions

The Goldslide intrusions occur extensively at Red Mountain, forming sills, dikes and irregular intrusive bodies which intrude the Triassic and lower parts of the Early Jurassic stratified sequences (Fig. 3). The Goldslide intrusions are all hydrothermally altered to some degree. The intrusions comprise three texturally and chemically distinctive phases, here termed the Hillside porphyry, the Goldslide porphyry and the Biotite porphyry. All phases locally contain a trachytic fabric outlined by hornblende phenocrysts that has variable orientation, but is generally subparallel to contacts.

Medium-grained hornblende + plagioclase porphyry, termed the Hillside porphyry, occurs extensively on the south ridge and the east side of Red Mountain as discordant intrusive bodies (Fig. 3). Phenocrysts are generally 1 mm to 3 mm long and comprise 10% to 20% acicular hornblende and 30% to 50% lath shaped plagioclase (Fig. 4). The latter commonly have rounded corners. The phenocrysts occur in an aphanitic groundmass. Amphibolite xenoliths, 0.5 cm to 4 cm wide, are locally common in these intrusions on the south ridge of Red Mountain.

The Goldslide porphyry is a hornblende-biotite ± quartz porphyry intrusion that underlies most of the Red Mountain cirque (Figs. 2 and 3). It comprises 5% to 15%, 2 mm to 10 mm long blocky hornblende phenocrysts and trace to 5%, 2 mm to 5 mm long biotite phenocrysts in a groundmass of fine-grained (typically <1 mm) equant plagioclase (35% to 50%) with an aphanitic matrix (Fig. 5). Quartz is locally present as 1 mm to 5 mm phenocrysts that are commonly rounded or embayed. Apatite is a common accessory mineral, and with plagioclase it is commonly encapsulated in hornblende phenocrysts. The Goldslide porphyry is distinguished from the Hillside porphyry by (1) the larger size and blocky habit of hornblendes, (2) small and equant plagioclase phenocrysts, and (3) the common presence of quartz and biotite phenocrysts. The presence of Goldslide porphyry dikes cross-cutting Hillside porphyry and xenoliths of Hillside porphyry within the Goldslide porphyry indicate that the Goldslide porphyry is the younger of the two phases.

Sills of Biotite porphyry intrude cherty sedimentary rocks on the west side of Red Mountain (Fig. 3). The Biotite porphyry (Fig. 6) is texturally similar to the Hillside porphyry, and contains approximately 5% to 15% acicular, 1 mm to 4 mm long hornblende phenocrysts, 20% to 35% plagioclase phenocrysts, and 1% to 5% blocky, 2 mm to 6 mm wide biotite phenocrysts within an aphanitic groundmass. It is distinguished from the Hillside porphyry by the presence of biotite phenocrysts and a greater proportion of groundmass, and from the Goldslide porphyry by the small size and shapes of the hornblende and plagioclase phenocrysts. No con-

FIGURE 6. Biotite porphyry.

FIGURE 7. Photograph of a contact breccia from the footwall of the Marc zone on section 1175N. Angular sedimentary rock fragments and subrounded Hillside porphyry fragments (tan to cream) occur in a granular tuffaceous matrix.

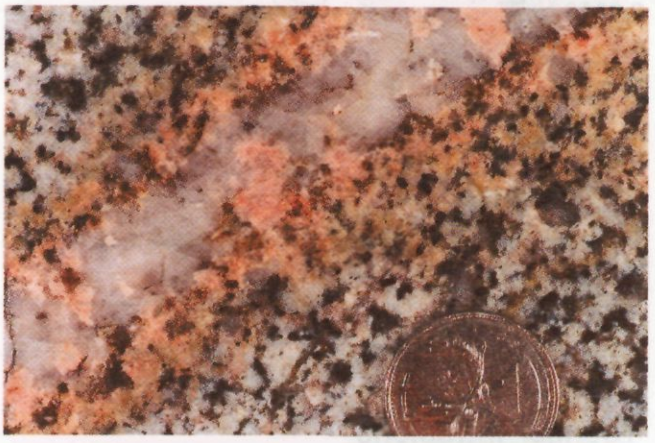

FIGURE 8. Photograph of the McAdam Point quartz monzonite stock. Note the quartz veinlet with a pink K-feldspar alteration envelope.

tact relationships with this unit and the Hillside porphyry or the Goldslide porphyry were observed.

K-feldspar occurs in the groundmass of all of the Goldslide intrusions but its origin is ambiguous, making classification of the intrusions difficult. K-feldspar content in least altered samples of the various phases is typically 15% to 25% in the Hillside porphyry, 15% to 20% in the Goldslide porphyry, and 20% to 30% in the Biotite porphyry. If the K-feldspar is primary, the mineralogy and geochemistry (Table 1) of the Goldslide intrusions indicate a compositional range from monzodiorite to quartz monzodiorite. Lower TiO_2 contents, and variation in $Na_2O + K_2O$ with respect to Fe_2O3 and MgO (Table 1) suggest that the Goldslide porphyry and Biotite porphyry are marginally more fractionated than the Hillside porphyry.

Contact features associated with the Goldslide intrusions, including intrusive breccias, breccia dikes and highly disrupted bedding, occur commonly on the east side of Red Mountain in the transition from the Triassic to the Early Jurassic sequences. These features are associated primarily with contacts of Hillside porphyry, and subordinately Goldslide porphyry, where they intrude probable Early Jurassic mudstone and siltstone beneath the summit of Red Mountain. The breccias include matrix- and fragment-supported varieties. Fragment abundance generally increases with proximity to the sedimentary country rock, particularly screens and rafts. The most fragment-rich breccias, commonly developed adjacent to sedimentary rafts, contain fragments of subround to angular mudstone/siltstone with or without round to subround Hillside porphyry fragments, all in a fine- to medium-grained crystalline to sandy tuffaceous matrix (Fig. 7). Locally, sedimentary fragments are plastically deformed and have irregular, lobate margins. Interlocking patterns between breccia fragments and between fragments and wallrock in some breccias suggest minimal transport. Near contacts with the sedimentary rocks (5 m to 10 m), the Hillside porphyry commonly has a texture resembling a fine- to medium-grained clastic or tuffaceous rock. Angular to subround fragments of mudstone/siltstone are present within the porphyry up to 25 m from rafts. Breccia contacts with both sedimentary rocks and intrusions vary between gradational and sharp. Widespread disruption of bedding occurs for up to 10 m to 30 m from the brecciated contacts. Highly lobate contacts between intrusions and sedimentary rocks, and detached apophyses of intrusions in the sedimentary rocks, occur locally where breccias are developed.

Breccia dikes and sills, commonly 1 cm to >2 m wide, are common near where the intrusive breccias occur. They emanate from the intrusions or contact breccia zones and intrude adjacent sedimentary wallrock, Hillside porphyry, contact breccias and/or other breccia dikes. The breccia dikes and sills are texturally similar to the contact breccias and contain fragments of sedimentary rocks, and subordinately, intrusions. Breccia dikes are also associated with the Hillside porphyry, and locally the Goldslide porphyry, on the east side of the south ridge, and with sills of Biotite porphyry near the toe of the Rio Blanco glacier.

The contact breccias and breccia dikes show alteration and veining typical of intrusive and sedimentary rocks at Red Mountain, and are therefore interpreted to predate hydrothermal activity. Brecciation occurs where the Goldslide intrusions intrude some of the youngest stratified rocks on Red Mountain. Common breccia dikes, tuffaceous textures in the intrusions near contacts, rounded intrusive fragments in some breccias, widespread disruption of bedding, and angular to plastically deformed sedimentary fragments are consistent with explosive phreatic activity related to igneous intrusion into wet, partially unconsolidated sediments (cf. Kokelaar, 1982). The stratigraphic position and similar age of the affected sedimentary rocks and the intrusions are consistent with this interpretation, which was previously suggested by Greig et al. (1994a, 1995). However, brecciation developed deeper within the Goldslide porphyry (>100 m from known contacts with sedimentary rocks) may be related to early magmatic-hydrothermal activity.

Early descriptions of the Hillside porphyry, based on short surface drill holes in the Marc zone where brecciation is common, refer to it as a crystal tuff (e.g. Vogt, 1991; Schroeter at al., 1992). Subsequent work indicates that it is intrusive and that sedimentary rocks originally regarded as tabular beds within the porphyry are actually isolated rafts (Fig. 10).

Clasts of the Goldslide porphyry, Hillside porphyry and Biotite porphyry in the overlying volcaniclastic sequence and the geochemical similarity of volcanic rocks and the Goldslide intrusions

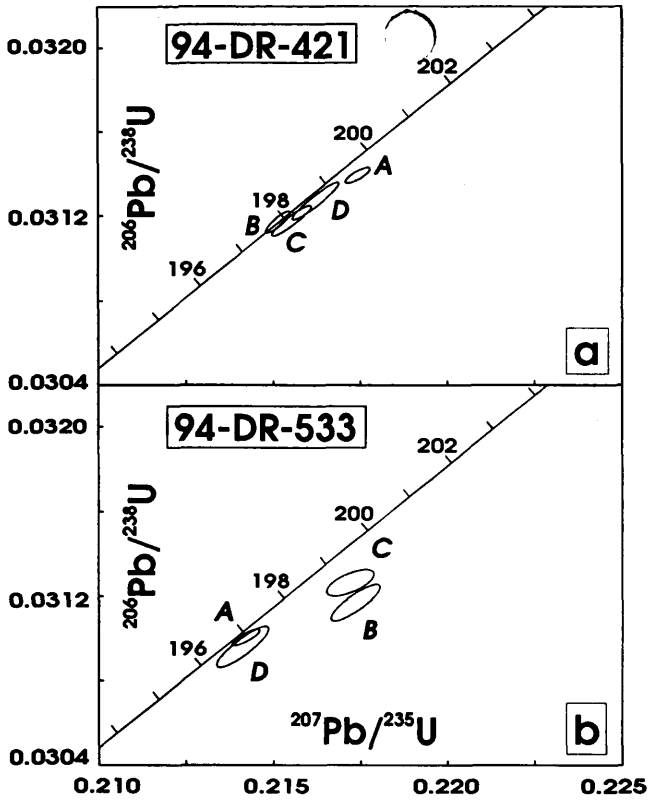

FIGURE 9. U-Pb concordia plots for zircon analyses from Goldslide porphyry.

suggest that the Goldslide intrusions are subvolcanic high level intrusions that were comagmatic with some of the volcanic rocks.

Younger Intrusions

The Tertiary McAdam Point stock and several types of mafic dikes intrude the Goldslide intrusions and all stratified rocks on Red Mountain. The McAdam Point stock is a 0.6 km 0.8 km wide intrusion that occurs at the south end of Red Mountain and extends across the east arm of Bromley glacier to Lost Mountain (Fig. 3). It is a medium- to coarse-grained biotite quartz monzonite (Fig. 8) with common K-feldspar megacrysts. Schroeter et al. (1992) report a 45 ± 2 Ma $^{40}Ar/^{39}Ar$ biotite date for the stock. The stock is associated with a 500 m to 800 m wide aureole of biotite hornfels that imparts a brown to purple tint to all pre-Tertiary rocks. Bedding-parallel pale green/tan and brown bands of calcite, actinolite, epidote, chlorite, and biotite, and local garnet are developed in sedimentary rocks adjacent to the stock, and suggest contact metasomatic activity.

Green, northeast-trending and steeply-dipping pyroxene porphyritic dikes occur in the Hillside Mountain cirque adjacent to Goldslide Creek. They intrude the Goldslide porphyry and screens within it, are typically 0.5 m to 4 m wide, and are magnetic. They contain <1% to 4%, 1 mm to 6 mm long blocky pyroxene phenocrysts that are commonly altered to amphibole in a fine-grained groundmass. The dikes cut quartz stockworks and alteration related to the Goldslide intrusions, but are cut by east-dipping quartz + calcite extension veins.

Dark grey to green, northwest-trending and steeply dipping trachyandesite dikes cut all other rocks on the property. Individual dikes are traceable for up to 2 km and vary from less than 5 cm to 7 m wide. Thinner dikes are green-grey, aphanitic and commonly flow banded. Thicker dikes commonly contain 0.5 mm to 3 mm long acicular amphibole phenocrysts and disseminated magnetite in a glassy, locally chloritzed, groundmass. Aphanitic chilled contacts are common. Dikes are spatially associated with, are parallel to, and locally intrude southwest-dipping gouge-filled faults. Similar dikes throughout the Stewart and Alice Arm areas are of middle Tertiary age (25 Ma to 40 Ma; Carter, 1981; Alldrick, 1993). Northeast-trending amygdaloidal, probably basaltic, dikes cut the trachyandesite dikes on Lost Mountain (K. Bull, pers. comm., 1994).

Several northwest-trending felsite sills and dikes occur on the lower western slopes of Red Mountain and on the low hills above Bromley glacier. They are commonly altered and pyritic, suggesting that they predate the Jurassic alteration event on Red Mountain.

Geochronology of Early Jurassic Units

Previous isotopic age determinations for Early Jurassic rock units in the Red Mountain area have been reported by Schroeter et al. (1992), Greig et al. (1995) and Greig and Gehrels (in press). Greig et al. (1995) obtained a K-Ar age of 194 ± 4 Ma for hornblende from andesitic pyroclastic rocks of the Hazelton Group about 2 km northwest of Red Mountain, and Greig and Gehrels (in press) obtained a U-Pb zircon age of 199 ± 2 Ma from andesite tuff about 5 km south of the mountain. Both age determinations were from rocks on strike, or correlative with, the green and maroon volcanic and volcaniclastic rocks that occur on the north side of Rio Blanco glacier and at the top of the Red Mountain stratigraphy (Fig. 3). Greig et al. (1995) also reported a U-Pb zircon age of 201.8 ± 0.5 Ma for a sample of Biotite porphyry 200 m west of the summit of Red Mountain (Fig. 3). Schroeter et al. (1992) reported $^{40}Ar/^{39}Ar$ ages of ~200 Ma and ~160 Ma for hornblende from two samples of the Goldslide porphyry southwest of the main adit (Fig. 3). It was suggested that the ~200 Ma age was close to the age of emplacement of the unit and the ~160 Ma age reflected a subsequent thermal disturbance.

Two samples were processed for U-Pb zircon dating from each of the Hillside and Goldslide porphyries, the two intrusive phases most intimately associated with mineralization. Samples weighing

TABLE 2. U-Pb analytical data

Sample description[1]	Wt (mg)	U (ppm)	Pb[2] (ppm)	$^{206}Pb/^{204}Pb$ (meas.)[3]	Total common Pb (pg)	% ^{206}Pb[2]	$^{206}Pb/^{238}U$[4] (± 1σ)	$^{207}Pb/^{235}U$[4] (± 1σ)	$^{207}Pb/^{206}Pb$[4] (± 1σ)	$^{207}Pb/^{206}Pb$ age (Ma; ± σ)
					Sample 94-DR-421					
A: N2, + 149,a	0.264	436	13.1	13720	16	5.4	0.03139 (0.06)	0.2174 (0.08)	0.05023 (0.04)	205.8 (2.1)
B: N2, + 149,a	0.390	546	16.5	16570	24	6.6	0.03117 (0.08)	0.2151 (0.08)	0.05006 (0.04)	197.6 (1.9)
C: N2, + 149,a	0.320	522	15.7	11430	29	6.6	0.03118 (0.12)	0.2155 (0.13)	0.05014 (0.05)	201.3 (2.2)
D: N2,105-149	0.109	520	15.9	7209	15	7.5	0.03127 (0.14)	0.2162 (0.16)	0.05015 (0.05)	202.0 (2.3)
					Sample 94-DR-533					
A: N2, + 149,a	0.117	468	13.9	4439	23	5.4	0.03101 (0.06)	0.2142 (0.09)	0.05011 (0.05)	199.9 (2.5)
B: N2, + 149,a	0.106	506	15.2	4326	23	5.8	0.03117 (0.14)	0.2174 (0.16)	0.05057 (0.08)	221.4 (3.9)
C: N2, + 149,a	0.130	542	16.4	2282	57	6.6	0.03126 (0.10)	0.2172 (0.16)	0.05039 (0.12)	212.9 (5.5)
D: N2, + 149,a	0.115	497	14.9	7844	13	6.3	0.03096 (0.16)	0.2141 (0.17)	0.05016 (0.08)	202.3 (3.8)

[1] N1, N2 = non-magnetic at given degrees side slope on Frantz isodynamic magnetic separator; grain size given in microns; a = abraded
[2] radiogenic Pb; corrected for blank, initial common Pb, and spike
[3] corrected for spike and fractionation
[4] corrected for blank Pb and U, and common Pb

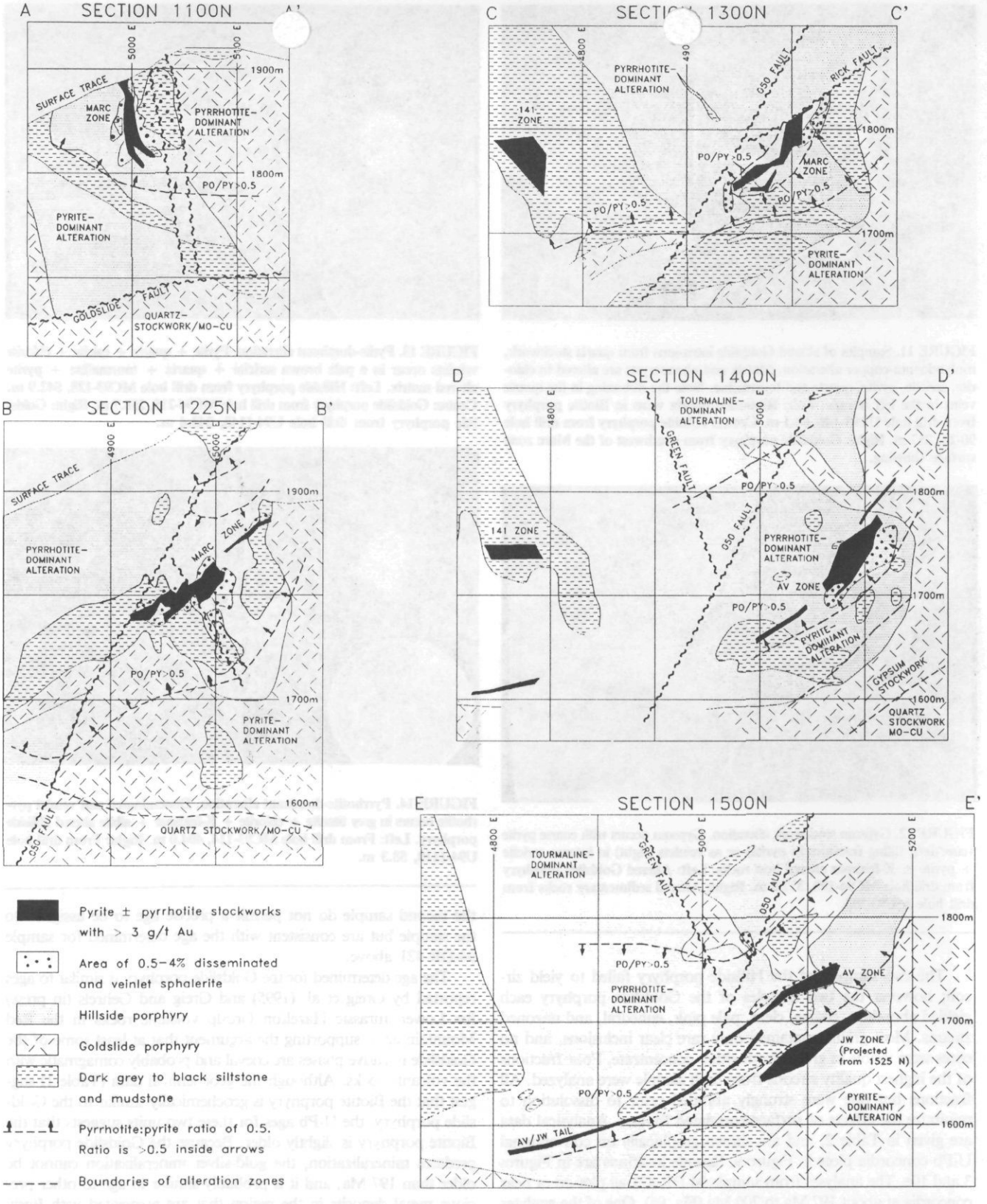

FIGURE 10. Cross-sections through the Marc, AV, JW, 141 and AV/JW Tail zones showing geology and alteration distribution. Views are to the northwest. The grid is in metres and elevations are in metres above sea level. Locations of the sections are shown in Figure 1 (inset). The pyrrhotite:pyrite ratio of 0.5 marks the boundaries of pyrrhotite-dominant alteration. Point X in E-E′ is the location of U-Pb zircon sample 94-DR-533, collected from underground.

from 25 kg to 30 kg were processed using conventional crushing, grinding, wet shaking table, heavy liquid and magnetic separator techniques. Techniques for final selection of zircon grains and methods for sample dissolution, chemical separation and purification of U and Pb, and mass spectrometry are those described by Mortensen et al. (1995).

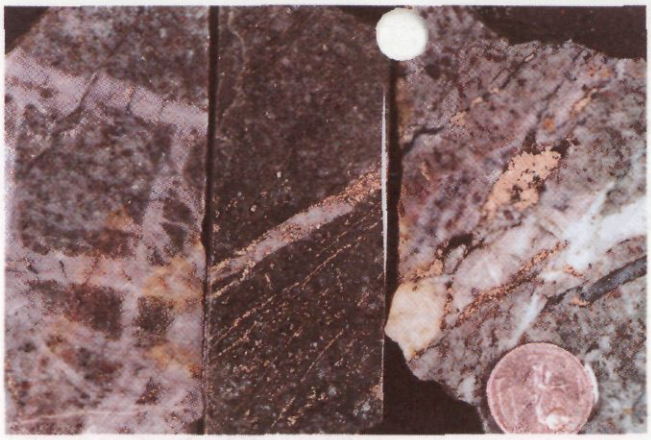

FIGURE 11. Samples of altered Goldslide intrusions from quartz stockwork, molybdenum-copper alteration. Matrix and phenocrysts are altered to chlorite, sericite, pyrite, quartz and tourmaline. Note the ribboning in the quartz veins in the left sample. Left: Ribboned quartz veins in Biotite porphyry from drill hole UT93-149, 64.1 m. Centre: Hillside porphyry from drill hole 90-28, 257 m. Right: Goldslide porphyry from southwest of the Marc zone surface showing.

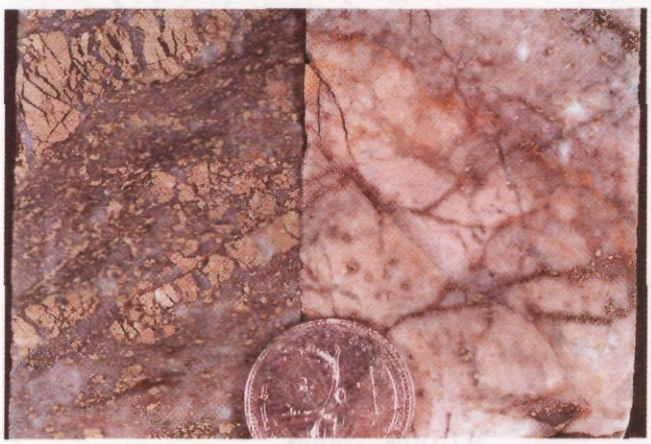

FIGURE 12. Gypsum stockwork alteration. Gypsum occurs with coarse pyrite veins (left, filling fractures in pyrite) or as veinlets (right) in intense sericite + pyrite ± K-feldspar altered host rocks. Left: Altered Goldslide porphyry from drill hole MC94-190, 377.9 m. Right: Altered sedimentary rocks from drill hole MC93-103.

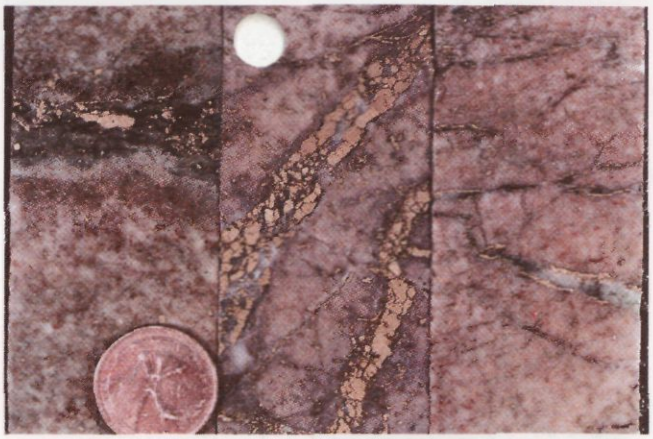

FIGURE 13. Pyrite-dominant alteration. Pyrite + quartz + calcite + chlorite veinlets occur in a pale brown sericite + quartz + tourmaline + pyrite altered matrix. Left: Hillside porphyry from drill hole MC93-128, 542.9 m. Centre: Goldslide porphyry from drill hole MC94-215, 258.7 m. Right: Goldslide porphyry from drill hole U94-1148, 243.4 m.

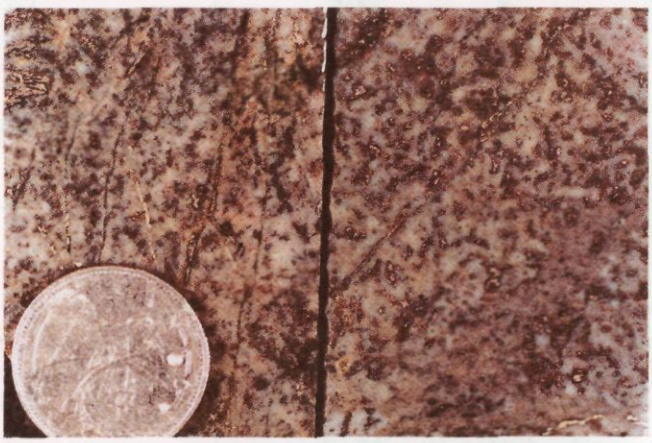

FIGURE 14. Pyrrhotite-dominant alteration. Disseminated and veinlet pyrrhotite occurs in grey titanite + chlorite + K-feldspar + albite altered Hillside porphyry. Left: From drill hole MC93-114, 404.0 m. Right: From drill hole U94-1110, 58.3 m.

The two samples of the Hillside porphyry failed to yield zircon; however the two samples of the Goldslide porphyry each yielded abundant, coarse, clear, pale pink, euhedral, and unzoned zircons. Most grains contained only rare clear inclusions, and no cores were visible in grains from either concentrate. Four fractions of the highest quality zircons from each sample were analyzed. All fractions but one were strongly abraded prior to dissolution to minimize the effects of surface-correlated Pb-loss. Analytical data are given in Table 2, and are shown graphically on conventional U-Pb concordia plots in Figure 9. Sample locations are in Figures 3 and 10e. The analyses from sample 94-DR-421 all plot on or near concordia at about 197 Ma to 200 Ma (Fig. 9a). One of the analyses (fraction B) is concordant with a $^{207}Pb/^{206}Pb$ age of 197.1 ± 1.9 Ma. This is considered to be the best estimate of the crystallization age of the sample. The other analyses give slightly older $^{207}Pb/^{206}Pb$ ages (up to 205.8 Ma; Table 2), which are interpreted to indicate the presence of a minor component of older, inherited zircon in three of the four analyses, likely as cryptic cores that were not distinguished visually. Four analyses from the second sample of the Goldslide porphyry are slightly discordant, with $^{207}Pb/^{206}Pb$ ages up to 221.4 Ma (Table 2, Fig. 9b). This may also indicate the presence of a minor component of inherited zircon. The data from the second sample do not permit a precise age to be assigned to the sample but are consistent with the age determined for sample 94-DR-421 above.

The age determined for the Goldslide porphyry is similar to ages reported by Greig et al. (1995) and Greig and Gehrels (in press) for Lower Jurassic Hazelton Group volcanic rocks in the Red Mountain area, supporting the argument that at least some of the Goldslide intrusive phases are coeval and probably comagmatic with the volcanic rocks. Although the geochemical data (Table 1) suggest that the Biotite porphyry is geochemically similar to the Goldslide porphyry, the U-Pb ages for these two units suggests that the Biotite porphyry is slightly older. Because the Goldslide porphyry predates mineralization, the gold-silver mineralization cannot be older than 197 Ma, and it is probably similar in age to other precious metal deposits in the region that are associated with Early Jurassic intrusions (e.g., Alldrick, 1993; Rhys, 1993).

Structural Geology

Structural features on Red Mountain are consistent with a deformation sequence involving early sulphide, quartz and calcite veins associated with the large mineralizing hydrothermal system, followed by at least one phase of folding, and displacement along northeast and northwest-trending faults. The early veins are described in the alteration section below.

FIGURE 15. Tourmaline vein stockwork. Tourmaline + pyrite + chlorite + pyrrhotite veins occur in K-feldspar + titanite + pyrite ± sericite altered Hillside porphyry. Acicular hornblende phenocrsyts are completely altered to brown aggregates of titanite + sericite + chlorite in the sample on the left. Left: From drill hole MC93-114, 316.5 m. Right: Collected from section 1475N, underground.

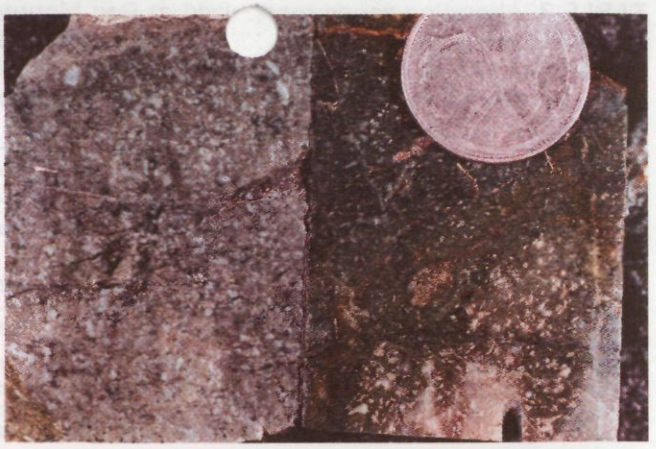

FIGURE 16. Actinolite alteration. Green to grey K-feldspar + actinolite + chlorite + titanite + albite alteration affects Hillside porphyry. Left: From drill hole MC93-128, 98.5 m. Right: From drill hole MC93-125, 115.2 m.

FIGURE 17. Laminated calcite + chlorite + sericite + pyrite + Fe-carbonate vein from drill hole U94-1120, 114 m.

Mesoscopic folds affect the entire Triassic/Jurassic succession on Red Mountain. Folds have moderate to steep north to northwest-plunging axes, generally steep limb dips, and open to tight, locally isoclinal, forms. Bedding is generally upright. Fold patterns are commonly complicated on the outcrop scale, especially near intrusive contacts, and are difficult to trace in the Triassic sedimentary rocks due to the difficulty of determining facing directions. Asymmetry of minor folds varies from clockwise on the west side of the mountain to counterclockwise on the east (Fig. 3), and together with bedding facing directions, suggests that the Bitter Creek antiform (Greig et al., 1994a, 1994b), runs from west of the exploration camp north past the west side of the Torresito Icefield (Fig. 3). West to southwest-dipping axial planar slaty cleavage that is defined by the preferred orientation of phyllosilicates and by pressure solution planes, is developed along the west slope of Red Mountain, within and west of the probable trace of the Bitter Creek antiform. The cleavage affects Triassic strata and the Hillside and Goldslide porphyries. It crenulates pyrite veinlets, but it is cut by the McAdam Point stock and related dikes and veins. Elsewhere, rocks are unfoliated, except near northwest-dipping shear zones (see below). The geometry and inferred timing of the folds and related foliation (post-Early Jurassic and pre-Tertiary) suggest that they are the local manifestation of Cretaceous-Early Tertiary Skeena Fold Belt deformation that affected the region (Evenchick, 1991; Greig et al., 1995).

Minor folds occurring in Early Jurassic strata near the summit of Red Mountain have axes which generally plunge to the northwest, typical of most folds on the mountain. Other folds in this area plunge to the northeast. The northeast plunging set, which include open to chevron style folds, are locally refolded by the northwest plunging folds (T. Calon, pers. comm., 1993), suggesting that they represent an older phase of folding. Map patterns in Figure 3 also suggest that broad, open, northeast-plunging folds may affect much of Red Mountain, but hinges were not observed at the outcrop scale. The age of this possible early event is bracketed by the strata they affect (Early Jurassic) and by the later folding event. However, the folds may also reflect complex strain patterns developed around the Goldslide intrusions during a single phase of progressive deformation and folding.

Moderately to steeply northeast- and southeast-dipping extension veins are common on the east side of Red Mountain. Veins are filled with blocky to fibrous calcite and quartz, and locally contain axinite, pyrrhotite, pyrite, clinozoisite and/or tremolite. The veins are lenticular, typically 0.5 cm to 5 cm wide, and are often developed in en echelon arrays. Axinite occurs where the veins cut alteration that contains tourmaline and actinolite (see alteration section below). West-dipping slaty cleavage is locally developed around en echelon extension vein arrays north of Rio Blanco glacier. Similar veins are found elsewhere in the Stewart area and in the Iskut River area to the north, and are locally associated with, and orthogonal to, west-dipping axial planar fabrics of regional north to northwest trending Cretaceous to Early Tertiary folds (P.D. Lewis, pers. comm., 1994).

At least two phases of faulting affect Red Mountain lithologies. The earliest faults are steep northwest-dipping semi-brittle shear zones that form prominent lineaments on Red Mountain. These structures include the Goldslide and Rick faults (Fig. 3, inset) that displace ore zones. They have phyllitic foliations defined by sericite and chlorite, and cataclastic textures such as rounded wallrock fragments in a cohesive, weakly-foliated, fine-grained, grey calcareous matrix. Oblique foliations, shear bands, slickensides on foliation surfaces, and displaced markers, including the ore zones, suggest that these structures have a right lateral sense of displacement with a normal component. Gouge seams developed in these structures indicate subsequent brittle movements. The timing of displacement with respect to folding is uncertain.

North to northwest trending, moderately to steeply southwest- and northeast-dipping faults are developed throughout the Red Mountain area and are locally associated with trachyandesite dikes. They cut the McAdam Point stock and all other structures, including northwest-dipping shear zones. The faults are typically filled with clay gouge, have bleached, argillically altered envelopes, and are associated with two phases of veining. Early ankerite + calcite +

TABLE 3. Alteration zones recognized at Red Mountain. Information is based on macroscopic observation by the authors and on petrography by Thompson (1994). The alteration types are overlapping and commonly gradational. Alteration is listed from highest (actinolite) to lowest (quartz stockwork, molybdenum-copper), and corresponds with decreasing elevation. The geochemistry is based on whole rock and ICP data from the Hillside porphyry and the Goldslide porphyry.

Alteration	Thickness	Geochemistry	Veins	Mineralogy of pervasive alteration
Actinolite dominant alteration	>150 m	MnO > 0.14%; Na_2O > 3.3%; K_2O < 0.5%; LOI < 3%; Sr > 400 ppm; SiO_2 < 56%; CaO > 2.8%	Chlorite + pyrite + actinolite + calcite	Green to grey K-feldspar + actinolite + chlorite + titanite + albite + pyrite (<1%) ± pyrrhotite (<.5%)
Tourmaline stockwork	100-300 m	MnO > 0.14%; Na_2O > 3.3%; K_2O < 0.5%; LOI< 3%; Sr> 400 ppm; SiO_2 < 56%; CaO > 2.8%	Tourmaline + pyrite + chlorite + pyrrhotite	Grey K-feldspar + chlorite + titanite + pyrite (<1%) + tourmaline + pyrrhotite (<0.5%); pyrrhotite:pyrite <0.5
Pyrrhotite-dominant alteration	100-200 m	MnO > 0.14%; Na_2O > 3.3%; K_2O <0.5%; LOI < 3%; Sr > 400 ppm; SiO_2 < 56%; CaO > 2.8%	Pyrrhotite + pyrite ± chalcopyrite ± chlorite ± calcite ± quartz ± sphalerite ± galena	Grey to brown-grey K-feldspar + sericite + pyrrhotite (<0.5%, commonly <.5%) + pyrite (<.5%) + chlorite ± tourmaline; pyrrhotite:pyrite <0.5
Auriferous pyrite + pyrrhotite stockwork[1]	10-50 m	K_2O >5%; Na_2O <1.5%; MnO < 0.1%; SiO_2 >54%; high values in Au (>0.5 ppm); Ag, As, Sb and locally Cu, Zn correspond with ore zones	Pyrite ± pyrrhotite ± quartz ± chlorite	Intense grey sericite + pyrite; mantled by disseminated and veinlet sphalerite + pyrrhotite + pyrite (2-20%); pyrrhotite:pyrite variable, usually <0.5
Pyrite-dominant alteration	100-200 m	SiO_2=52-56%; MnO < 0.1%; Na_2O < 3.5%; K_2O > 4%; LOI > 3%; Sr <100 ppm; CaO < 3.3%	Pyrite ± calcite ± quartz ± chlorite	Cream to tan sericite, pyrite (>2%) ± calcite ± chlorite ± tourmaline; pyrrhotite:pyrite <0.5
Gypsum stockwork[2]	<5-100 m	Similar to pyrite-dominant alteration	Gypsum + pyrite + calcite ± quartz	Pale grey sericite + pyrite (>1%) ± quartz ± K-feldspar
Quartz stockwork, molybdenum-copper	>200 m	Cu > 300 ppm; Mo > 30 ppm; SiO_2 >55% and similar values to pyrite dominant alteration for MnO, Na_2O, K_2O, CaO, LOI and Sr	Quartz + pyrite ± chlorite ± epidote ± magnetite ± molybdenite ± chalcopyrite	Green to grey sericite + quartz + pyrite (>1%) + chlorite + K-feldspar ± epidote ± tourmaline ± magnetite ± hematite

[1]Locally developed at the top of the quartz stockwork, molybdenum-copper alteration
[2]Locally developed at or above the transition from pyrite- to pyrrhotite-dominant alteration

quartz + pyrite ± arsenopyrite ± galena ± sphalerite veins commonly occur within the faults or in their immediate wallrocks. The veins often intersect the faults obliquely and have steeper dips. Together with shallow dipping cleavage in some faults, this suggests a normal sense of displacement (cf. Helmstaedt, 1991). The Fe-carbonate veins are cut by vuggy calcite + quartz + pyrite veins that locally seal fault gouge. Steep-dipping gouge fabrics and cleavage that disrupt Fe-carbonate veins in faults and displaced markers indicate late reverse movements on some of these faults (e.g. the 050 Fault, Fig. 10c).

East-west trending, steeply dipping non-penetrative cleavage is locally developed in Triassic cherty sedimentary rocks and Biotite porphyry sills north of the exploration camp. Its significance and relationship to other structures was not ascertained.

Alteration and Mineralization Related to the Goldslide Intrusions

Hydrothermal alteration affects pre-Tertiary rocks on Red Mountain, including all phases of the Goldslide intrusions. The red colour of the mountain results from the widespread development of iron oxides after disseminated and veinlet pyrite and pyrrhotite.

Porphyry-style quartz stockwork veins associated with weak molybdenite ± chalcopyrite mineralization and propylitic alteration are developed within the Goldslide porphyry throughout the cirque and in sills of Biotite porphyry north of the exploration camp and beneath the summit (Figs. 3 and 11). K-feldspar, sericite, pyrite, chlorite, epidote and molybdenite often occur in the quartz veins or in envelopes. Mafic phenocrysts are commonly altered to actinolite, chlorite, titanite, magnetite, hematite and pyrite. Groundmass and plagioclase phenocrysts are commonly replaced by or contain disseminated sericite, epidote, quartz, K-feldspar and pyrite. Quartz veins are locally sheeted but typically form stockworks. Veins vary from 0.3 cm to 4 cm in width and are spaced 0.2 m to 1 m apart. Stockwork quartz veins are locally cut by pyrite, epidote, chlorite ± magnetite veinlets, and rarely, molybdenite ± pyrite veinlets. Alteration intensity increases to the east in the stockwork zones, where it becomes texturally destructive. Disseminated tourmaline is developed locally in this area as well.

Quartz stockwork veins extend from exposures in the cirque to beneath the summit of Red Mountain where they occur within the Goldslide porphyry near its upper contact and extend into adjacent Hillside porphyry. In this area, several shallowly northwest-dipping alteration zones are developed above the quartz stockwork veins (Figs. 3 and 10). These outcrop west of the surface exposure of the Marc zone on the north side of the cirque and in the valley of Rio Blanco Creek (Fig. 2). The alteration zones are subparallel to the upper contact of the Goldslide porphyry. The quartz stockwork molybdenum-copper alteration passes up into successive alteration assemblages that are characterized by the presence of gypsum veins, pyrite, pyrrhotite, tourmaline veins and actinolite (Table 3). They are generally gradational over 5 m to 30 m, but boundaries can be abrupt. Vein mineralogy generally reflects the pervasive alteration mineralogy suggesting that they formed together. An expansive volume of gold mineralization (>0.3 g/t gold) occurs at or just above the transition from pyrite- to pyrrhotite-dominant alteration over a >1 km^2 area that is 10 m to 100 m thick (Figs. 3 and 10a, 10b and 10d). Higher grade gold-silver mineralization in pyrite stockwork veins associated with more intense alteration occurs within the area of anomalous gold and locally projects upward into higher alteration zones (Table 3). These higher grade stockworks are described in the following section.

Gypsum ± calcite ± pyrite ± quartz stockwork veins and veinlets are developed locally over thicknesses of 20 m to 100 m at the top of the molybdenum-copper zone, below the AV zone, and typically within the Goldslide porphyry (Fig. 10d). The veins occur within intense, pale grey coloured sericite ± K-feldspar alteration (Fig. 12). Coarse pyrite (>5 mm grains) occurs in many veins. The top of the gypsum stockwork is commonly broken and rubbly, due to the dissolution of gypsum veins.

Pyrite-dominant alteration occurs above the gypsum and quartz stockworks and is characterized by >2% disseminated and veinlet

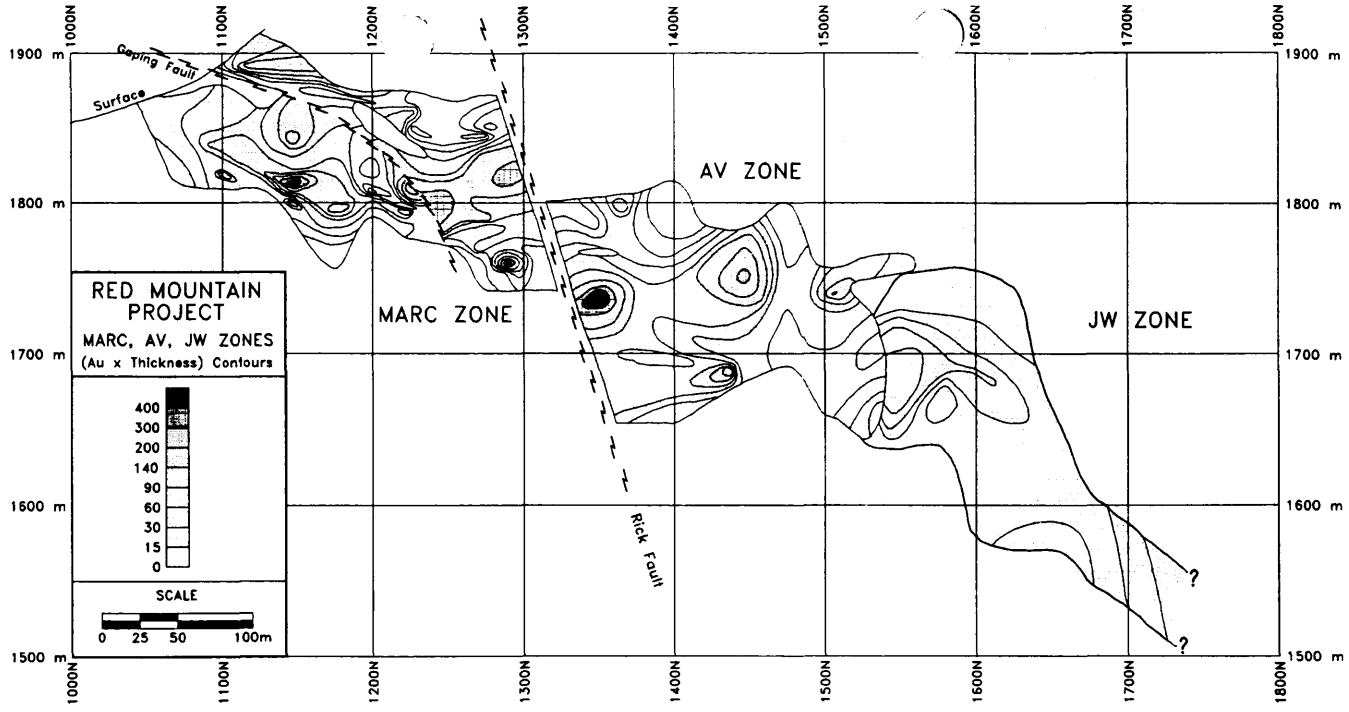

FIGURE 18. Vertical long section of the Marc, AV and JW zones, looking southwest. Contours are of gold (g/t) x thickness (m). View is to the southwest.

pyrite in an intensely pyrite + sericite + quartz ± K-feldspar ± calcite-altered cream to pale grey matrix. It varies in thickness from 70 m to 200 m wide and extends upward from the Goldslide porphyry into the Hillside porphyry and the host sedimentary rocks (Fig. 10). Coarse pyrite (generally >2 mm grains) ± quartz ± calcite ± sericite ± chlorite veins and veinlets are abundant and are typically 1 mm to 15 mm wide, but are locally up to 0.6 m wide. Vein envelopes of chlorite, sericite and locally pale brown tourmaline, are common (Fig. 13). Alteration is usually associated with disseminated blebs of pyrite ± chlorite ± brown tourmaline ± titanite that replace mafic phenocrysts (Thompson, 1994; Fig. 13). Titanite, K-feldspar and tourmaline are most abundant near the top of the pyrite alteration. Vein gold grades are highly variable in the pyrite zone, and veins typically contain <1 g/t Au, although values up to 14 g/t occur locally.

Pyrrhotite-dominant alteration occurs within the Hillside porphyry and sedimentary rafts above the pyrite-dominant alteration (Fig. 10). It is typically 100 m to 200 m thick and is characterized by >0.5% disseminated and veinlet pyrrhotite, with pyrrhotite:pyrite ratios >0.5 (Fig. 10). Pervasive K-feldspar + chlorite + titanite + pyrrhotite ± pyrite ± carbonates ± albite alteration imparts a grey brown colour to this zone (Fig. 14). Disseminated tourmaline in blebs with sulphides is locally common. Pyrrhotite ± pyrite ± chlorite ± calcite ± chalcopyrite ± sphalerite ± galena ± arsenopyrite veins 0.3 cm to 2 cm, and locally >15 cm in width are developed with variable intensity throughout the zone. Where intersected in underground workings the veins dip steeply to the west. Gold grades in pyrrhotite veins within the pyrrhotite zone typically range between 0.5 and 6 g/t Au.

Above the pyrrhotite-dominant alteration, pyrrhotite:pyrite ratios generally drop to <0.5, and pyrrhotite abundance decreases to <0.5%. The pyrrhotite alteration is succeeded by alteration containing tourmaline ± pyrite ± pyrrhotite ± chlorite ± sericite ± sphalerite veins, generally 0.1 cm to 5 cm wide, that occur widely spaced in stockworks (Figs. 10d and 10e: tourmaline stockwork, and Fig. 15). Tourmaline is brown to black, commonly euhedral and typically encapsulated in pyrite grains. Pervasive K-feldspar + chlorite + titanite ± sericite + pyrite ± tourmaline alteration is similar to that of the pyrrhotite zone, and imparts a pale green to grey colour (Fig. 15; Thompson, 1994). Tourmaline + pyrite veins commonly contain 0.05 g/t to 0.3 g/t Au.

Actinolite-K-feldspar alteration (actinolite-dominant alteration) is the highest alteration zone developed on Red Mountain (Fig. 16), and is developed above the tourmaline stockwork. Rocks are altered to a pale green colour by the effects of pervasive actinolite + K-feldspar + chlorite + pyrite + calcite + albite + pyrrhotite alteration. Titanite and actinolite commonly replace mafic phenocrysts (Thompson, 1994).

The alteration is affected by two late phases of veining. In the quartz stockwork/molybdenum-copper, pyrite and ore zones, fibrous quartz + chlorite + muscovite + calcite fills fractures in coarse pyrite within veins, occurs in pressure shadows in veins, or occurs in discrete, narrow (<4 mm) veinlets distal to pyrite veins. Oblique and rotated fibres indicate minor displacements. The fibrous veinlets are cut by laminated calcite + quartz + sericite + pyrite + chlorite veins and veinlets (Fig. 17). Younger veins of this type, defined by cross-cutting relationships, are progressively enriched in calcite. The laminated veins contain minerals characteristic of the alteration that they occur in, and have alteration envelopes consistent in mineralogy with older veins in each alteration zone, suggesting that they are related to, but late, in the development of the alteration. Foliation is usually developed in these veins and is defined by compositional layering, phyllitic laminae of sericite and chlorite, and by shape fabrics in calcite. Where intersected underground, the veins dip moderately to steeply southeast to northeast. Oblique foliation, the orientation of calcite fibres, and offset older veins suggest a component of reverse simple shear. Chlorite + pyrite stringers that occur throughout the underground workings may be related to these veins.

The alteration weakens in intensity laterally to the southwest, where the alteration zonation is poorly developed in the cherty rocks that predominate there. In the Red Mountain cirque, the valley of Rio Blanco Creek and under the Cambria Icefield to the northeast, the zoned alteration is truncated by erosion. Alteration transects stratigraphy, affecting Early Jurassic conglomerates in the Cambria zone and the lowermost green trachyandesitic tuffs under the Cambria Icefield northeast of the mountain. Sedimentary rocks with a porcelaneous white appearance that probably results from

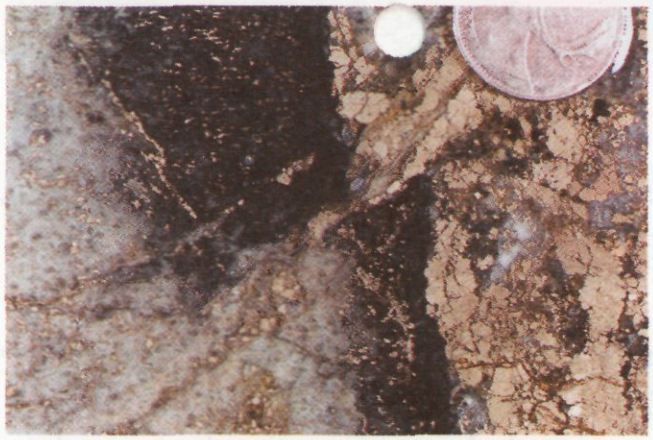

FIGURE 19. Marc zone vein. Coarse pyrite + quartz + chlorite vein in strongly sericite-altered Hillside porphyry from the Marc zone, 1295N crosscut. Note the chlorite envelope on the vein, and the alteration of plagioclase phenocrysts in the porphyry to grey, irregularly shaped aggregates of sericite. A calcite + pyrite stringer (bottom left of the coin) cuts the vein and displaces it.

recrystallization (Thompson, 1994), and local silicification of intrusions and country rock are common on the west side of Red Mountain where Goldslide intrusions intrude cherty rocks.

Gold-Silver Pyrite-Pyrrhotite Stockwork Mineralization

The majority of the mineral inventory at Red Mountain is contained within three semi-tabular to elliptical, shallow northwesterly plunging and southwest dipping pyrite stockwork zones: the Marc zone, the AV zone and the JW zone (Figs. 3, 10 and 18). They form a 700 m long, broadly continuous trend of mineralization which is bounded on the southeast by the Goldslide Fault (Fig. 3) and is still open to the northwest. The remaining resources occur in the down-dip extension of the AV and JW zones, termed the AV/JW Tail, and in the 141 zone. All of these resources occur at or just above the anomalous gold zone, near the transition between pyrite- and pyrrhotite-dominant alteration and 100 m to 200 m above the quartz stockwork with molybdenum-copper mineralization. The boundaries of the zones are based on an assay cutoff of 3 g/t Au over a minimum of 3 m, and there are no apparent distinct lithologies or bounding structures which define them. These assay control boundaries do not always reflect the actual shape of the pyrite stockworks.

The Marc, AV and JW zones are mainly developed within the Hillside porphyry, and to a lesser extent, in brecciated sedimentary rafts. The ore zones typically occur within 100 m of the Goldslide porphyry, within or just above a linear embayment in its margin (Fig. 10). The embayment contains two large and elongate rafts of sedimentary rocks separated by Hillside porphyry, resulting in a funnel shape (Figs. 10a and 10b). This geometry is best developed in the area of the Marc zone and western portions of the AV zone. Contact breccias are extensively developed in the embayment, especially along the margins of the Hillside porphyry. Brecciation is also common in the underlying Goldslide porphyry.

The Marc zone, the only ore zone exposed at surface, crops out at the 1900 m elevation, 300 m southeast of the summit of Red Mountain at the head of the Red Mountain cirque (Figs. 2 and 3). It is a crudely tabular zone that dips moderately to steeply to the southwest. The zone lies primarily within Hillside porphyry between the two rafts of sedimentary rocks, and virtually bridges the gap between the two sides of the embayment in the Goldslide porphyry (Figs. 10a, 10b and 10c). Where the zone intersects sedimentary rocks on its lower (southwest) end, the sulphides are less abundant and gold grades are more erratic. At its upper (northeast) end, the Marc zone thins and the gold grade is lower, terminating at or near the contact with the Goldslide porphyry.

The AV zone is offset 100 m from the Marc zone by the northwest-dipping semi-brittle Rick Fault (Figs. 3 and 18). The AV zone is of similar thickness and grade as the Marc zone (Table 4, Fig. 18). In the vicinity of the AV zone, the embayment in the Goldslide porphyry widens, and sedimentary rafts within it become more discontinuous (Fig. 10). The AV zone is more tabular and dips more shallowly than the Marc zone (Figs. 10d and 10e). It lies approximately 50 m to 75 m above the Goldslide porphyry. Like the Marc zone, the gold grade and continuity of the AV zone decreases at its lower (southwest) end where it intersects sedimentary rafts. However, upper portions of the AV zone are commonly well developed within brecciated sedimentary rafts. A dike of Goldslide porphyry forms the upper bound to part of the AV zone, although the zone transects the dike on its northwestern end. Although the AV zone has been traced by drilling as far northwest as section 1600N (Fig. 18), pyrite content and gold grades decrease dramatically at section 1525N. The mineralized zone thereafter is expressed as veinlet and disseminated sphalerite ± pyrrhotite.

The JW zone, which dips more shallowly and is thinner (Table 4) than the Marc and AV zones, is the most northwesterly of the ore zones at Red Mountain (Figs. 3, 10e and 18). Its southeastern end occurs 50 m below the northwestern termination of the AV zone on section 1525N at a point where the top of the Goldslide porphyry drops a corresponding amount. The transition from the AV to the JW zones zone thus reflects the morphology of the porphyry, because both zones are developed approximately 50 m to 75 m above it. Like the Marc and AV zones, the JW zone is associated spatially with brecciated rafts of sedimentary rocks.

The Marc, AV and JW zones consist of a stockwork of coarse pyrite veins, veinlets, breccia veins and pervasively disseminated pyrite, mainly in pale grey strongly sericite altered Hillside porphyry (Figs. 19 and 20), or, less commonly, in adjacent tan to pale green sericite-altered mudstone and siltstone. The pyrite veins commonly contain up to 15% quartz and less than 5% chlorite, pyrrhotite, sphalerite and/or chalcopyrite. Vein widths range from less than 0.5 cm up to 1 m, but are typically less than 3 cm. Veins are variably spaced, commonly 2-10 per m, and usually comprise less than 5% or 10% of any drill intersection (Fig. 20). Veins in the stockworks have general moderate to steep southwest- and northeast-dipping orientations. Dark green chlorite envelopes are commonly

TABLE 4. Average thickness and selected geochemistry of gold-silver pyrite stockwork zones on Red Mountain, based on drill data. N is the number of drill intersections used in calculations. Data is from representative drill holes in the zones and does not represent all of the intersections. The same drill intersections were used to generate Figure 18.

Zone	True thickness (m)	Strike length (m)	Dip length (m)	Maximum thickness (m)	N	Au (g/t)	Ag (g/t)	Zn (ppm)	Cu (ppm)	As (ppm)	Sb (ppm)	Ag:Au
Marc	12.3	275	150	24.0	97	11.5	45.3	1494.1	479.9	455.9	147.0	4.0
AV	14.9	225	150	29.2	34	10.3	29.0	842.5	915.5	666.9	310.0	2.8
JW	6.2	250	250	11.0	18	8.2	15.2	1062.2	298.8	335.0	38.8	1.8
AV/JW Tail	4.1	150	350	6.0	14	4.9	9.6	1311.8	1347.2	185.9	27.2	2.0
141	20.0	100	100	46.8	11	4.3	6.9	506.8	892.5	221.3	20.0	1.6

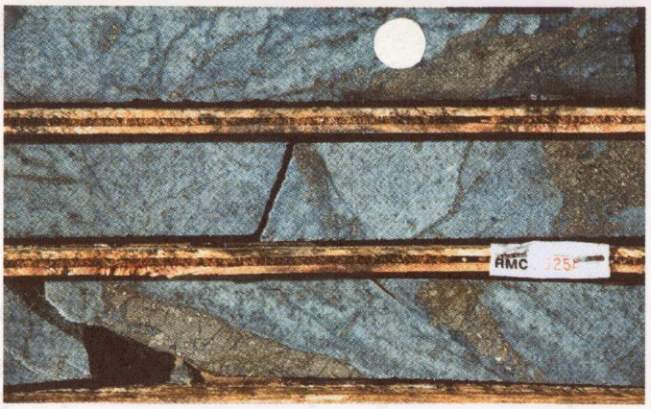

FIGURE 20. Typical drill intersection of the Marc zone. Coarse pyrite veins occur in intensely sericite altered Hillside porphyry. The core is 4 cm in diameter. From drill hole UG93-1075, 73 m to 76 m.

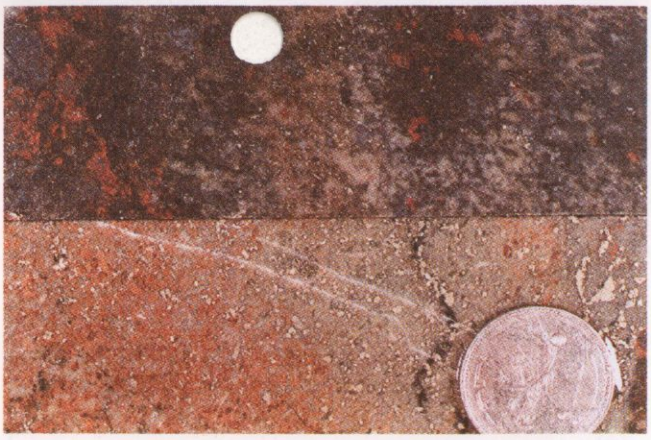

FIGURE 21. Sphalerite halo to the AV (top) and Marc (bottom) zones. Disseminated red sphalerite in sericite + titanite + K-feldspar + chlorite + pyrrhotite-altered Hillside porphyry. The darker colour of the top sample results from abundant disseminated chlorite with the sphalerite. Top: From drill hole U94-1117. Bottom: From drill hole U93-1022, 57.5 m.

developed on pyrite veins (Fig. 19). Vein pyrite is very coarse (generally 1 mm to 20 mm wide) and commonly fractured. Fractures are filled with narrow seams of fibrous quartz, muscovite, calcite and chlorite.

Gold, silver, copper, arsenic, lead and antimony are enriched in the ore zones (Table 4). Pyrite veins typically grade 3 g/t Au to >100 g/t Au. Gold occurs in grains of native gold (typically 0.5 to 15 microns, rarely up to 2 mm), petzite, electrum (commonly >20% Ag), and various gold tellurides and sulphosalts (Ford, 1993; Barnett, 1991). Native gold and gold-bearing minerals occur with silver tellurides along cracks in pyrite grains, within fibrous quartz-muscovite filled fractures in pyrite, and subordinately, as inclusions in pyrite (Barnett, 1991; Rodd, 1990). Other gold- and silver-bearing minerals include hessite, tetrahedrite, muthamannite, calaverite, aurostibite, altaite, montbrayite, krennerite and sylvanite (Barnett, 1991; Rodd, 1990; Ford, 1993). Native gold occurs locally in chlorite.

The Marc, AV and JW zones are partially surrounded by an aureole of disseminated and veinlet sphalerite ± pyrrhotite that is developed for 2 m to 50 m into both the footwall and hanging-wall, but it is typically thicker in the footwall (Fig. 10). Red to yellow sphalerite, generally 0.5% to 4%, occurs disseminated and in veinlets with pyrrhotite (commonly >5%) and pyrite (Fig. 21). Associated gold grades are typically 0.3 g/t to 2.0 g/t. Sphalerite is generally more concentrated in screens of black sedimentary rocks than in the Hillside porphyry, and occurs preferentially in coarser-grained beds. Pervasive alteration is similar to the surrounding area of pyrrhotite-dominant alteration (Table 3). The transition from alteration in the sphalerite halo to the pervasive sericite-pyrite alteration and pyrite veining in the ore zones is abrupt and commonly occurs over intervals of less than 1 m.

Examination of the Marc, AV and JW zones in drill core and in underground workings indicates that they have no bounding structures, except where late structures, such as the Rick Fault and northwest-trending gouge-filled faults, displace or intersect them. The only pervasive fabrics that occur in the ore zones are local trachytic, sericite-altered hornblende phenocrysts, and phyllitic foliation developed in postmineralization shear zones, or in narrow, late alteration laminated calcite veins.

Other Mineralized Pyrite-pyrrhotite Veins and Stockworks

Gold mineralization continues on the down-dip, western extension of the AV and JW zones, joining to form the AV/JW Tail zone (Fig. 10e). It comprises two parallel, shallowly southwest-dipping, tabular zones that occur between sections 1425N and 1575N at the top of the anomalous gold horizon. The AV/JW Tail zone occurs primarily within the Hillside porphyry 50 m above the top of the Goldslide porphyry (Fig. 10e). It is commonly developed at or near the margins of sedimentary rafts. Alteration is similar to that in the Marc, AV and JW zones, but sphalerite is not typically developed adjacent to this zone.

The 141 zone is 200 m southwest of the Marc and AV zones, at approximately the same elevation (Figs. 10c and 10d). It is developed primarily in altered sedimentary rocks at the top of the anomalous gold horizon, at and above the contact with the Hillside porphyry. It locally extends into the underlying Hillside porphyry and occurs approximately 70 m to 120 m above the Goldslide porphyry, or above dikes of Goldslide porphyry (Figs. 10c and 10d). Mineralization consists of a stockwork of pyrrhotite + pyrite ± chalcopyrite ± chlorite veins and veinlets that are associated with intense sericitic alteration in the Hillside porphyry or with porcelain-textured quartz ± sericite alteration in the sedimentary rocks. Pyrrhotite is generally more abundant than pyrite in the altered sedimentary rocks, and pyrite is most abundant in the Hillside porphyry. Disseminated and veinlet sphalerite occurs locally.

Other precious metal showings on Red Mountain (Fig. 3) reflect local increases in the intensity of sulphide veining and alteration. The Cambria zone occurs in Lower Jurassic conglomerates east of the Marc zone showing (Fig. 3) and comprises steeply dipping, northeast and northwest trending, pyrite extension veins with chlorite envelopes. The Brad zone is an area of pyrite veining associated with intense sericitic alteration and fibrous tourmaline which overprint quartz stockwork veins. The Singh and Silver Shear showings occur within cherty sedimentary rocks on the south ridge and are 3 m to 5 m wide zones of subparallel, steep north dipping quartz + calcite + pyrrhotite + pyrite + sphalerite + chalcopyrite + galena + molybdenite veins with K-feldspar alteration envelopes. The Meg zone is a broad area of moderate to intense alteration which locally contains auriferous (commonly >1 g/t Au) stockworks of pyrrhotite + pyrite veins.

Mineralization Related to the McAdam Point Stock

At the south end of Red Mountain and on Lost Mountain, porphyry-style molybdenum and gold mineralization is associated with the McAdam Point stock (Fig. 3). Quartz veins and veinlets occur throughout the stock and in country rock within 50 m of its contacts. The veins either trend northeast with steep dips or dip steeply southwest. Veins commonly have well-developed, green to grey muscovite alteration envelopes, or have envelopes of coarse, pink K-feldspar with outer muscovite (Fig. 8). Pyrite, molybdenite,

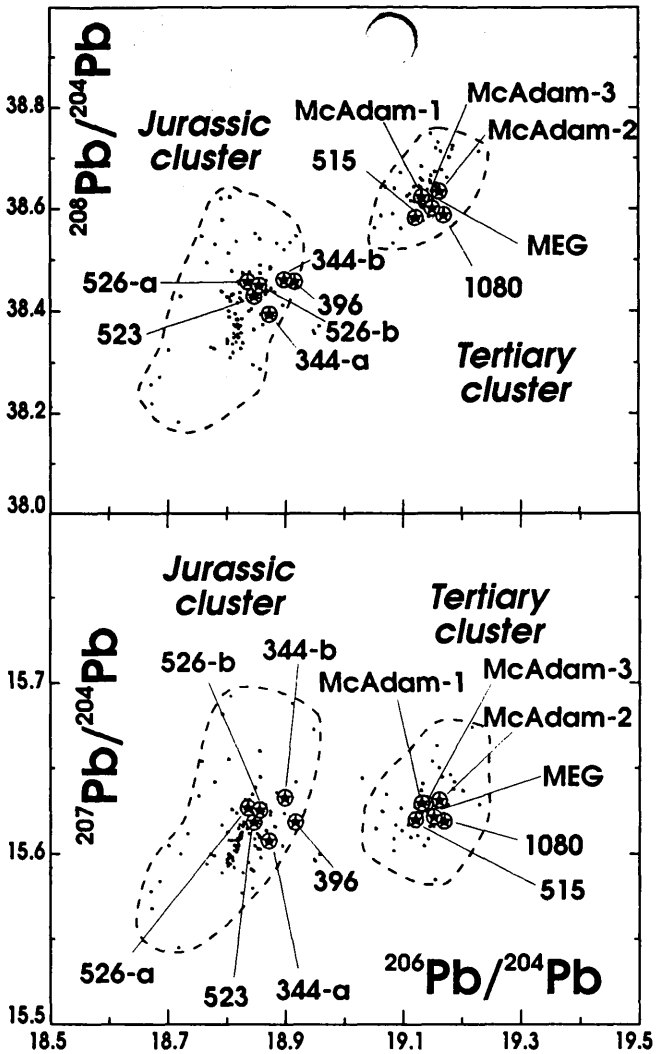

FIGURE 22. Plots of lead isotopic data for galena, pyrite and feldspar from the Red Mountain area.

and more rarely, chalcopyrite occur disseminated in the veins, on vein selvages or in the alteration envelopes. On Lost Mountain, veins are typically 0.5 cm to 4 cm wide and are generally widely spaced (>2 m), although they occur locally in densities of up to 5/m. Larger veins are developed within the stock on the south side of Red Mountain. Here, several 0.2 m to 1 m wide, 30 m to 100 m long steeply west-southwest-dipping quartz-pyrite veins are developed. These veins commonly greater than 30% pyrite, with subordinate sphalerite, chalcopyrite and galena, and are enriched in gold (up to 46 g/t; Vogt, 1991). Like quartz-molybdenite veins, the auriferous quartz-pyrite veins have K-feldspar ± muscovite alteration envelopes. In the contact aureole of the stock, quartz-molybdenite veins are absent, and irregular actinolite + calcite + diopside + chlorite + epidote veins, which commonly have bleached white to pink albite envelopes, are locally abundant. They are of similar orientation to the veins developed in the stock.

Dating and Lead Isotopic Studies of Alteration and Mineralization

Dating of alteration associated with gold-silver mineralization on Red Mountain was attempted using K-Ar methods. Most alteration minerals are too fine-grained to be concentrated sufficiently for dating purposes; however, alteration envelopes up to 1 cm wide, characterized by intense sericitization, are locally developed around pyrite veins below the precious metal zones. A sample of a sericite

TABLE 5. K-Ar analytical data for a sericitic pyrite vein envelope from dri[illegible]re in the pyrite-dominant alteration zone (section 1400, drill hole MC93-130, 500.1 m)

Sample	K (wt%)	Rad ^{40}Ar cc/gm 10^{-6}	Rad $^{40}Ar/^{40}Ar$	Age ± 2 σ (Ma)
Sericitized vein envelope	5.97	23.4	83.2	98.1 ± 5.8

envelope on a pyrite vein from beneath the AV zone in pyrite-dominant alteration (section 1450N, drill hole MC93-130, 500.1 m) was dated by K-Ar whole rock methods at the Geochronology Laboratory at The University of British Columbia. The analytical techniques that were used generally follow those described by Greig et al. (1992). Analytical data are given in Table 5. The age of 98.1 ± 5.8 Ma obtained for this sample is interpreted to reflect partial thermal resetting of the alteration sericite, possibly by the same event(s) that disturbed the $^{40}Ar/^{39}Ar$ age spectra of analyses reported by Schroeter et al. (1992). Although disturbed, the Early Cretaceous age gives a minimum age for the mineralization on Red Mountain, and argues against a genetic relationship between the mineralization in the ore zones and the hydrothermal system associated with the Tertiary McAdam Point stock.

Lead isotopic compositions were measured for galena, pyrite and feldspar from a variety of mineral occurrences and their host rocks on Red Mountain in order to help constrain the timing and origin of the deposit. Godwin et al. (1991) and Alldrick et al. (1993) demonstrated that the lead isotopic compositions of galenas provide an effective geochemical discriminant between mineral occurrences associated with Early Jurassic intrusions in the Stewart and Iskut River areas and those associated with Early Tertiary intrusions, and their data define two distinct clusters in lead isotopic space. Lead isotopes were measured for galena samples from veins in pyrrhotite-dominant alteration above the AV zone, the Singh showing, and three late, base-metal-bearing, calcite and iron carbonate vein occurrences that are associated with gouge-filled faults on Red Mountain. Trace lead isotopic compositions were measured for pyrite from stringers within the molybdenum-copper zone, pyrite from stockwork veins within the Early Tertiary McAdam Point stock, unaltered K-feldspar phenocrysts from the McAdam Point stock, and K-feldspar alteration envelopes on quartz stockwork veins in the McAdam stock. Analytical data are given in Table 6, and are plotted in Figure 22. Outlines of the Early Jurassic and Early Tertiary clusters are from Godwin et al. (1991) and Alldrick et al. (1993). The lead isotopic compositions of galena from pyrrhotite veins above the AV zone, galena from the Singh showing, and pyrite from the copper-molybdenum stockwork style of mineralization in the Red Mountain cirque clearly fall within the main Early Jurassic field. However, lead isotopic compositions of galena from late carbonate veins, trace lead from quartz-pyrite veins within the McAdam Point stock and trace lead from feldspars in the stock are similar and plot in the Tertiary field (Fig. 22). This argues that the intense alteration zones and related gold-silver mineralization and the Singh showing on Red Mountain are Early Jurassic in age and likely related to the Early Jurassic Goldslide intrusions, and that late, base metal-bearing veins in the area are of Early Tertiary age, possibly developed peripherally to small Early Tertiary intrusions such as the McAdam Point stock.

Discussion and Conclusions

The interpreted geologic history of the Red Mountain area is summarized in Table 7. The age, geochemistry and stratigraphic position of the Goldslide intrusions suggests that they may be coeval and comagmatic with the overlying Early Jurassic volcanic rocks, and that the intrusions are subvolcanic. The Goldslide porphyry is the youngest phase of the Early Jurassic intrusions recognized on Red Mountain.

TABLE 6. Lead isotopic compositions of galena, pyrite and K-feldspar fr[illegible] the Red Mountain area

Sample No.[1]	Description	$^{208}Pb/_{2}$ Pb	$^{207}Pb/_{2}^{204}Pb$	$^{208}Pb/_{2}^{204}Pb$
94-DR-523	Pyrrhotite alteration, galena in pyrrhotite vein	18.846	15.619	38.429
94-DR-526-a	Pyrrhotite alteration, galena in pyrrhotite vein	18.836	15.627	38.457
94-DR-526-b	Duplicate of 94-DR-526-a	18.856	15.626	38.449
94-DR-344-a	Singh showing, galena from sulphide vein	18.872	15.608	38.394
94-DR-344-b	Duplicate of 94-DR-344-a	18.899	15.633	38.460
94-DR-396	Pyrite veinlet in molybdenum-copper zone	18.909	15.619	38.463
94-DR-515	Fe-carbonate vein with galena in gouge-filled fault	19.122	15.620	38.582
MEG	Fe-carbonate vein with galena in gouge-filled fault	19.150	15.623	38.599
UG1080, 44 m	Late Fe-carbonate + galena + sphalerite vein	19.171	15.619	38.589
McAdam-1	K-feldspar megacrysts, McAdam Point stock	19.131	15.624	38.623
McAdam-2	Pyrite veinlet in the McAdam Point stock	19.136	15.621	38.615
McAdam-3	K-feldspar envelope, quartz vein, McAdam Point stock	19.160	15.625	38.637

[1]bold letters correspond to labels in Figure 9
[2]all errors are <.01% at a 2 level

TABLE 7. Geologic history of the Red Mountain area

Age	Event
mid Tertiary (25-40 Ma)	Intrusion of northwest-trending trachyandesite dikes, commonly into gouge-filled faults.
Tertiary	Formation of northwest-trending, predominantly southwest-dipping gouge-filled faults and associated calcite and Fe-carbonate veining.
Early Tertiary (45 Ma)	Intrusion of the McAdam Point stock, horfelsing of country rock and subsequent development of a potassic molybdenum-bearing hydrothermal system.
Cretaceous or Early Tertiary	Folding about northwest-trending, predominantly southwest-dipping axial planes, development of a parallel axial planar fabric on the west side of Red Mountain, and formation of east-dipping quartz ± calcite ± epidote ± pyrrhotite ± axinite extension veins. This event is probably related to regional Skeena fold belt deformation. Formation of northwest-dipping semi-brittle shear zones may pre- or postdate this event.
Early Jurassic (approx. 201 Ma to approx. 196 Ma)	Intrusion of the Goldslide intrusions and related volcanism in the following sequence: (i) Intrusion of the Biotite porphyry. (ii) Intrusion of the Hillside porphyry. (iii) Intrusion of the Goldslide porphyry. (iv) Formation of a zoned hydrothermal system with broad K-silicate alteration and gold deposition in semi-tabular pyrite + pyrrhotite stockwork zones. Early Jurassic volcaniclastic sedimentation and trachyandesitic volcanism are probably broadly synchronous with intrusion and mineralization.
Triassic to Early Jurassic	Deposition of cherts, cherty siltstone and mudstone and later (?Early Jurassic) fine- to coarse-grained clastic rocks.

Mineralization and alteration on Red Mountain is spatially associated with, but affects all phases of, the Goldslide intrusions. Lead isotopic compositions of sulphides associated with alteration on Red Mountain are similar to sulphide lead isotopic compositions from other deposits in the area that are Early Jurassic in age (e.g., Alldrick, 1993), and to lead isotopic compositions of K-feldspar phenocrysts in Early Jurassic intrusions (M.L. Bevier and J. Mortensen, unpubl. data). Where west-dipping axial planar fabrics are developed, pyrite veinlets are folded and Goldslide intrusions are foliated, indicating that both intrusions and mineralization are pre-kinematic with respect to regional deformation. Intrusions and alteration are also cut by east-dipping extension veins that are probably related to regional folding. Thus, the timing of mineralization relative to intrusions and folding, its stratigraphic position, close relationship to, and well-developed alteration zoning outward from the Goldslide porphyry, and lead isotopic signature of sulphides in the alteration zones are consistent with an Early Jurassic mineralizing event related to the Goldslide porphyry intrusion. These relationships also suggest that gold-silver mineralization and alteration occurred in a subvolcanic environment at the top of the Goldslide intrusions and just below the transition from Triassic sedimentary rocks to Early Jurassic volcanic rocks.

Anomalous gold mineralization (>0.3 g/t) is developed at the transition from pyrite- to pyrrhotite-dominant alteration. Highest gold-silver grades are associated with pyrite + pyrrhotite stockwork veins in intense sericitic alteration that are mantled by disseminated and veinlet sphalerite + pyrrhotite. The mineralized zones occur in the upper part of the anomalous gold horizon, generally <100 m above the top of the Goldslide porphyry, and extend up into the pyrrhotite-dominant alteration. They are associated with embayments and inflections in the Goldslide porphyry contact and occur where the anomalous gold horizon intersects brecciated bodies of siltstone and mudstone that are encapsulated in, or occur at the margins of, the Hillside porphyry. The sedimentary rocks may have had a two-fold effect: (1) as a permeability barrier to the movement of hydrothermal fluids that caused fluid overpressuring and stockwork veining, and (2) in reducing the hydrothermal fluids with resultant deposition of sulphides and gold. There are no bounding structures to the precious metal mineralization, and the morphology of the mineralized zones may instead be influenced by the overall trend of contrasting lithologies. Pyrite in veins in several of the alteration zones is affected by late fibrous veinlets and fractures filled with quartz, muscovite, calcite and chlorite. In the ore zones, these late fractures contain a significant proportion of the gold. They are in turn cut by calcite shear veins and veinlets that occur throughout the alteration zones and represent the final stages of alteration.

Although porphyry mineralization in the McAdam Point stock is similar to the quartz stockwork veins that are associated with the Goldslide porphyry, differences in (1) host intrusion age, (2) alteration style and extent, (2) isotopic signature, (4) timing with respect to regional deformation and (5) age of alteration on Red Mountain (98.1 ± 5.8 Ma K-Ar minimum age of sericite; Table 5), indicate that the Tertiary McAdam Point stock hydrothermal system is significantly younger than, and unrelated to, the main areas of alteration and mineralizationon Red Mountain. The composition, size, age, associated biotite hornfels, and porphyry-molybdenum mineralization of the McAdam point stock are typical of the Alice Arm intrusions which occur commonly for up to 50 km south and southeast of Red Mountain (cf. Carter, 1981).

The overall distribution and style of alteration on Red Moun-

tain is similar to that of many porph[illegible] systems. Like other systems, alteration at Red Mountain is co[illegible] quartz stockwork zones associated with molybdenum-copper mineralization, it has locally developed gypsum stockworks, and is boron-rich. Sericite and K-feldspar are widespread and alteration is zoned outward from a hornblende + biotite porphyritic intrusion, the Goldslide porphyry. However, the auriferous pyrite stockwork zones that comprise the ore zones are unusual compared to traditional porphyry systems. In British Columbia, the geologic setting and age of gold deposits on Red Mountain is comparable to other gold deposits in the Stewart area (e.g. Silbak Premier; Alldrick, 1993) and the Iskut River area to the north, which contains the Snip mine (Fig. 1; Rhys, 1993). Precious metal deposits at both Red Mountain and Snip are peripheral to subvolcanic Early Jurassic intrusions that have large related hydrothermal systems, and mineralization occurs near the transition from Triassic sedimentary rocks to Early Jurassic volcanic rocks. Early Jurassic intrusions with associated alteration that occur near this stratigraphic transition are thus prospective targets for Red Mountain, Snip and Silbak Premier style deposits. The Red Mountain deposits are developed in areas of well-developed alteration zoning where iron sulphide oxidation state changes.

Acknowledgments

Papers such as this one benefit from the accumulated knowledge gained by geologists over years of exploration. Those in particular who have contributed to the understanding of Red Mountain geology include the following Lac Minerals/Bond Gold staff and consultants: R. Barnett, A. Bray, K. Bull, T. Calon, D. Cawood, S. Creighton, P. Daubeny, C. Ford, I. Foreman, T. Hinderman, T. Hurley, P. Lutyinski, R. McLeod, G. MacVeigh, P. Pelletier, C. Russell, B. Singh, A. Thompson, A. Tuthill, A. Vogt, R. Walker, J. Watkins and G. Wober. Discussions with and work by C. Greig of the Geological Survey of Canada have been invaluable. The authors thank the staff of the Geochronology Laboratory at The University of British Columbia, especially Anne Pickering, for assistance in producing the isotopic analyses for this study. The paper was reviewed by K. Bull, C. Greig, P. Lhotka, C. Rockingham, A. Thompson and J. Thompson. This paper is dedicated to the memory of Andreas Vogt, Red Mountain project geologist, who died tragically near Red Mountain in 1991. The AV zone is named in his memory.

REFERENCES

ALLDRICK, D.J., 1993. Geology and metallogeny of the Stewart mining camp, northwestern British Columbia. British Columbia Ministry of Energy, Mines and Petroleum Resources, Bulletin 85, 105 p.

ALLDRICK, D.J., GODWIN, C.I. and SINCLAIR, A.J., 1993. An exploration application for lead isotope ratios, Stewart mining camp, northwestern British Columbia. Exploration and Mining Geology, 2, No. 2, p. 121-128.

ANDERSON, R.G., 1993. A Mesozoic stratigraphic and plutonic framework for northwestern Stikinia (Iskut River area), northwestern British Columbia, Canada. *In* Mesozoic Paleogeography of the Western United States. *Edited by* G. Dunne and K. McDougall. Society of Economic Paleontologists and Mineralogists, Volume II, Pacific Section.

BARNETT, R.L., 1991. Petrographic-metallurgical electron microprobe investigation of selected samples (20) from the Red Mountain Prospect, British Columbia. Unpublished company report, Lac Minerals Inc., Vancouver, British Columbia, 65 p.

CARTER, N.C., 1981. Porphyry copper and molybdenum deposits, west-central British Columbia. British Columbia Ministry of Energy, Mines and Petroleum Resources, Bulletin 64, 150 p.

CORDEY, F. and GREIG, C.J., 1995. Radiolarians from Red Mountain strata and environs, Nass River area. Cordilleran Geology and Exploration Roundup, Vancouver, British Columbia, Poster Presentation.

DOWNING, B.W. and LEITCH, C., 1980. Reconnaissance work, 1979, Stewart Area. Unpu[illegible]l company report, Falconbridge Nickel Mines Ltd., Vancouver, B[illegible]n Columbia, 33 p.

EVENCHICK, C.A., 1991. Structural relationships of the Skeena fold belt west of the Bowser Basin, northwestern British Columbia. Canadian Journal of Earth Sciences, 28, p. 973-983.

FORD, C., 1993. Gold characterization and metallic mineralogy of Red Mountain heads and residues. Unpublished company report, Lac Minerals Inc., Toronto, Ontario, 32 p.

GODWIN, C.I., PICKERING, A.D.R. and GABITES, J.E., 1991. Interpretation of galena lead isotopes from the Stewart-Iskut area. *In* Geological Fieldwork 1990, British Columbia Ministry of Energy, Mines and Petroleum Resources, Paper 1994-1, p. 235-243.

GREIG, C.J., ARMSTRONG, R.L., HARAKAL, J.E., RUNKLE, D. and VAN DER HEYDEN, P. 1992. Geochronometry of the Eagle plutonic complex and the Coquihalla area, southeastern British Columbia. Canadian Journal of Earth Sciences, 29, p. 812-829.

GREIG, C.J., ANDERSON, R.G., DAUBENY, P.H., BULL, K.F. and HINDERMAN, T.K., 1994a. Geology of the Cambria icefield: Regional setting for Red Mountain gold deposit, northwestern British Columbia. *In* Current Research 1994-A. Geological Survey of Canada, p. 45-56.

GREIG, C.J., ANDERSON, R.G., DAUBENY, P.H. and BULL, K.F., 1994b. Geology of the Cambria icefield area, northwestern British Columbia. Geological Survey of Canada, Open File 2931.

GREIG, C.J. and GEHRELS, G.E., in press. U-Pb zircon geochronology of Lower Jurassic and Paleozoic Stikinian strata and Tertiary intrusions, northwestern British Columbia. Canadian Journal of Earth Sciences.

GREIG, C.J., MCNICOLL, V.J., ANDERSON, R.G., DAUBENY, P.H., HARAKAL, J.E. and RUNKLE, D., 1995. New K-Ar and U-Pb dates for the Cambria icefield area, northwestern British Columbia. *In* Current Research 1995-A. Geological Survey of Canada, p. 97-103.

GROVE, E.W., 1968. MoS_2. British Columbia Department of Mines, Annual Report, 1967, p. 36-38.

HELMSTAEDT, H., 1991. Structural study of the Red Mountain property, Lac/Bond Gold Canada Inc., Skeena Mining Division, Stewart, British Columbia. Unpublished company report, Lac Minerals Inc., Vancouver, British Columbia, 16 p.

KOKELAAR, B.P. 1982. Fluidization of wet sediments during the emplacement and cooling of various igneous bodies. Journal of the Geological Society of London, 139, p. 21-33.

MORTENSEN, J.K, GHOSH, D.K. and FERRI, F., 1995. U-Pb geochronology of intrusive rocks associated with copper-gold porphyry deposits in the Canadian Cordillera. *In* Porphyry Deposits of the Northwestern Cordillera of North America. *Edited by* T.G. Schroeter. Canadian Institute of Mining, Metallurgy and Petroleum, Special Volume 46.

REEVE, A.E., 1967. Geological and geochemical investigation of the MoS_2 claim group, Skeena Mining Division, British Columbia. Unpublished company report, Erin Explorations Ltd., N.P.L., Vancouver, British Columbia, 11 p.

RHYS, D.A., 1993. Geology of the Snip mine and its relationship to the magmatic and deformational history of the Johnny Mountain area. Unpublished M.Sc. thesis, The University of British Columbia, Vancouver, British Columbia, 278 p.

RODD, K., 1990. Petrographic analysis of samples from the Marc zone, Red Mountain, British Columbia, Canada. Unpublished company report, Bond Gold Canada, Vancouver, British Columbia, 36 p.

SCHROETER, T., LANE, B. and BRAY, A., 1992. Geologic setting and mineralization of the Red Mountain mesothermal gold deposit. *In* Exploration in British Columbia 1991. British Columbia Ministry of Energy Mines and Petroleum Resources, Paper 1992-1, p. 117-125.

THOMPSON, A., 1994. Report No. 5 — Summary of alteration mineralogy, Red Mountain project, Stewart, British Columbia. Unpublished company report, Lac Minerals Inc., Vancouver, British Columbia, 6 p.

VOGT, A., 1991. Internal report (1990) on geological, geophysical, geochemical and diamond drill program at the Red Mountain and Bria Wotan property, Skeena Mining Division. Unpublished company report, Bond Gold Canada, Vancouver, British Columbia, 66 p.